5-2012

Exploring the Possibility of Floating Orbits for Extreme Mass Ratio Binary Black Holes

Shasvath Jagat Kapadia
University of Arkansas, Fayetteville

EXPLORING THE POSSIBILITY OF FLOATING ORBITS FOR EXTREME MASS RATIO BINARY BLACK HOLES

EXPLORING THE POSSIBILITY OF FLOATING ORBITS FOR EXTREME MASS RATIO BINARY BLACK HOLES

A thesis submitted in partial fulfillment
of the requirement of the degree of
Master of Science in Physics

By

Shasvath Jagat Kapadia
Indian Institute of Technology, Delhi
Master of Science in Physics, 2009

May 2012
University of Arkansas

Abstract

A binary black hole system, where each black hole orbits the system's center of mass, loses energy by emission of gravitational waves. This causes both black holes to spiral in towards each other. However, if the binary were to, by some mechanism, gain orbital energy at the same rate that it radiates away this energy, a non-decaying or "floating" orbit would result. The thesis uses superradiant scattering and tidal friction, which are two equivalent ways of looking at a process by which the system can gain orbital energy from the spin energy of either black hole, to determine the possibility of a floating orbit. It turns out that, for extreme mass ratio binary black holes in circular equatorial orbits, the energy radiated away comfortably exceeds the combined energy gained from the spin of both black holes. Thus, the thesis concludes that circular equatorial floating orbits generated via superradiant scattering/tidal friction are not possible.

This thesis is approved for recommendation
to the Graduate Council.

Thesis Director:

Dr. Daniel Kennefick

Thesis Committee:

Dr. Julia Kennefick

Dr. Reeta Vyas

Dr. Yo'av Rieck

Thesis Duplication Release

I hereby authorize the University of Arkansas Libraries to duplicate this thesis when needed for research and/or scholarship.

Agreed_____

Shasvath Jagat Kapadia

Refused_____

Shasvath Jagat Kapadia

Acknowledgement

This project has been my first real experience in original research work involving general relativity, and I have my adviser Dr. Daniel Kennefick to thank for giving me this opportunity. I enjoyed working with Dr. Kennefick, especially because of his willingness to discuss ideas in a warm, friendly and pressure free environment.

I would like to thank the Physics Department here at the University of Arkansas for giving me a strong base in core areas of physics and the confidence in my ability to do physics research.

And finally, I would like to express my sincerest and most heartfelt gratitude to my parents who have always been there supporting me, even in the most trying times.

Dedication

I offer this work to The Mother and Sri Aurobindo.

Contents

List of Figures

1 Introduction

1.1 Motivating the Floating Orbit

The motivation for the idea of the floating orbit can be traced back to a paper by J. Weber in 1970 who reported intensity measurements of gravitational waves that seemed to be emanating from a source at the center of the galaxy [1]. Even though these observations were the subject of great controversy, C.Misner, in 1970, came up with several theoretical models for the source that could be emitting these waves, carefully examining the plausibility of each of these models [2]. The conceptual origin of the floating orbit can be found within one of these theoretical models.

Weber tried to interpret these observations by proposing that this source isotropically emitted gravitational quadrupole radiation with a power of $10^3 M_\odot c^2/yr$ and frequency $\omega = 10^4 Hz$ [2]. However, if this were true, the entire galaxy ($10^{11} M_\odot$ [8]) would have been completely consumed by the source within $(10^{11} M_\odot)/(10^3 M_\odot/yr) = 10^8 yr$, which is 1% of its current age of about 10^{10} years [7],[2]. In fact, Sciama et al pointed out that any mass loss rate of above $70 M_\odot/yr$ over 10^8 years would affect the motion of stars and gas within the galaxy in a way that can be observed [6].

Misner concluded that the radiation could not be isotropic. He suggested gravitational synchrotron radiation (GSR for short). GSR is similar to electromagnetic synchrotron radiation (ESR). ESR occurs when a charged particle, whose acceleration and relativistic velocity are perpendicular to each other, emits radiation in a cone of narrow opening angle. The axis of the cone aligns with the direction of motion of the source [3]. The angular spread of GSR is similarly limited. An example of such a source would be a particle orbiting a central body at relativistic speeds.

Suppose the GSR source motion were approximately confined to the galactic plane, and the opening angle were $\Delta\theta$ with respect to the galactic plane, the area swept out by the cone as the source particle completes an orbit would be about $(r\Delta\theta)(2\pi r) = 2\pi\Delta\theta r^2$, where r is the distance from the source to the sun. The source power would now be reduced by a factor of $2\pi\Delta\theta r^2/4\pi r^2 \sim \Delta\theta$. Misner estimated $\Delta\theta$ to be about 10^{-3}. The GSR source power would therefore drop to $10^3 M_\odot c^2/yr \times 10^{-3} = 1 M_\odot c^2/yr$. Thus, only $10^{10} yr \times 1 M_\odot/yr = 10^{10} M_\odot$, or, 10% of the galaxy would have been used up by the source by the time the galaxy reaches its current age, assuming the source were active since the birth of the galaxy [2].

$\Delta\theta \sim 10^{-3}$ is a reasonable estimate for the GSR angular spread, given that the distance from the sun to the galactic center ($\sim 9kpc$ [4]) is far greater than the distance from the sun to the galactic plane ($\sim 26pc$ [5]).

Even a power of $1 M_\odot c^2/yr$ would require a large central body. This would conflict with Weber's measurement of the quadrupole radiation frequency of $\omega = 10^4 Hz$. Say, for example, that the body had a mass

of $M = 10^8 M_\odot$. The closest that the source particle can possibly orbit is roughly $R = 2GM/c^2$. This is because, closer than this radius, the particle cannot move fast enough to remain in a stable orbit. The source motion frequency cannot therefore exceed $w_o = c/R \sim 10^{-3} Hz$. Clearly then, the graviational wave frequency must be a higher harmonic of the source frequency, i.e $\omega = n\omega_o$, $n >> 1$. This is also a property of the GSR, since synchrotron radiation is dominated by higher multipole ($n >> 1$) harmonics.

GSR thus solves the problems of large source power and low gravitational radiation frequency associated with Weber's model trying to explain his results.

Among the various GSR source models that Misner examined (all of which proved to be unsatifactory [2]), he considered the floating orbit (Misner never actually gave it that name, but it is fairly clear that he came up with the idea).

1.2 Attempts at finding the Floating Orbit: Superradiant Scattering

Suppose the source were a particle in circular orbit around a rapidly spinning Kerr black hole. GSR would require the particle to have relativisitic speeds, and would therefore emit gravitational waves to infinity with a large power. If there were no mechanism by which the particle could get back the energy it loses to these waves, it would be unable to maintain a fixed orbit and would rapidly spiral into the black hole as its orbit decayed. Misner proposed the emission of negative energy gravitons down the Kerr black hole, which is equivalent to the particle extracting spin energy from the hole. While this would compensate for the energy lost to infinity, Misner believed the process would not last long enough to allow the particle to sustain its synchrotron orbit [2].

The first clear definition of the floating orbit was given by Press and Teukolsky in a paper submitted to Nature in 1972 "[...]orbits in which a particle radiatively extracts energy from the hole at the same rate as it radiates energy to infinity; thereby, it experiences net zero radiation reaction" [9]. The process by which the particle extracts the energy from the hole is called "superradiant scattering" (a term introduced by Press and Teukolsky) in which the gravitational waves reflected off the rotating Kerr black hole are more energetic than the incident ones, the excess energy coming at the expense of the black hole's spin energy.

Can such an orbit exist? Using Teukolsky's formalism in which the particle is treated as a perturbation in the Kerr metric [10], S.Detweiler was able to come up with an equation for the gravitational wave flux emitted by the particle in a circular orbit around the Kerr black hole [11]. Teukolsky's formalism was further employed by Glampedakis and Kennefick to determine the gravitational wave flux emitted by the particle to infinity and the black hole for eccentric orbits, thereby calculating precisely the nature of the inspiral of the particle orbiting the Kerr black hole [12]. They found that the flux down the hole was in fact negative, that superradiant scattering was occurring. However, this flux was a mere 10% of the flux emitted to infinity,

and therefore not nearly enough to sustain a floating orbit.

1.3 Attempts at finding the Floating Orbit: Tidal Friction

In a paper published in 1972, J.Hartle was able to show that when a particle (mass $m << M$) orbits a slowly rotating black hole (Kerr parameter $a << 1$) with a large constant orbital radius (circular equatorial orbit with $R >> M$), the black hole spins down, thus losing its spin energy to the particle's orbital energy [13]. Later work by Poisson et al extended Hartle's result to the cases of a black hole with arbitrary spin ($0 < a < 1$) orbiting in the weak graviational field ($R >> M$) of another arbitrary mass M_{ext} [16]; a small spinning black hole with Kerr parameter b ($0 < b < 1$) orbiting a large non-spinning black hole ($a = 0$; $m << M$) with radius greater than the ISCO (Innermost Stable Circular Orbit) radius ($R > R_{ISCO}$) [16]; and a small spinning black hole orbiting a large spinning black hole, with no restrictions on either spin ($0 < a < 1$; $0 < b < 1$; $m << M$), and the orbital radius greater than the ISCO radius ($R > R_{ISCO}$) [17]. Note that in the cases that have a smaller spinning black hole , only the spin energy lost by the small hole was calculated. To our knowledge, there is no known expression for the spin energy lost by the larger black hole in the tidal friction paradigm.

There is a close analogy between Hartle's and Poisson's results and the tidal interaction that occurs between a planet and its satellite; hence the name "tidal friction" [13]. In fact, K.Thorne, in his book titled "The Membrane Paradigm", suggested that the event horizon of a black hole may be looked at as a viscous membrane that gets distorted under the influence of an external mass, and in the process influences the orbital motion of that external mass [14].

In the light of this analogy, tidal friction may be interpreted as follows:
As the particle orbits the Kerr black hole, it causes bulges, which are distortions in the shape of the event horizon, to appear at diametrically opposite ends of the black hole. If the angular speed of the bulge is greater than that of the orbiting particle, the bulge exerts a torque on the particle, causing it to speed up, or equivalently, increasing its orbital energy [15]. The particle also exerts a torque on the bulge, thus slowing the angular speed of the black hole and dissipating the hole's rotational energy.

We shall show in a later section that tidal friction proves to be ineffective to establish a floating orbit, since the rate of loss of orbital energy to infinity via gravitational waves far exceeds the rate of gain of energy through tidal interaction.

1.4 Attempts at finding the Floating Orbit: Combining both Approaches

To maximize the possibility of a floating orbit, both black hole and particle must have spin, so that the spin energy of each may be converted to orbital energy of the system.

Superradiant scattering was used to examine the spin energy lost by the large spinning black hole to the orbital energy of the binary. Tidal friction was used to calculate the spin energy lost by the small spinning black hole to the orbital energy of the binary. The central point of this thesis is to add both these energy rates and compare it to the rate of energy lost to infinity via gravitational waves. It turns out once again that the energy loss rate to infinity comfortably exceeds both rates of gain of spin energy combined.

It has been suggested (though to our knowledge not formally proven) that tidal friction and superrradiant scattering are just two ways of looking at the same mechanism [12], [15]. Strong evidence of this will be provided in a later section. This definitively annulls the possibility of a floating orbit for a system of spinning extreme mass ratio binary black holes, since there is no other plausible mechanism by which the binary may compensate for the energy it radiates away.

2 A Short Primer On Orbits Around Rotating Black Holes

The purpose of this section is to introduce certain concepts and equations of general relativity (without detailed derivations), and, in particular, of orbits around spinning black holes. These equations will be referred to and used throughout the rest of the sections.

Note that, unless otherwise specified, all equations in this section have been taken from J. Hartle's book titled "Gravity" [21]. These equations are standard established equations in general relativity.

2.1 The Einstein Equation

In spite of its mathematical complexity, general relativity is based on an elegant and simple idea. Any matter-energy source causes spacetime to curve, and the trajectory of test particles (particles that are by themselves insignificant sources of spacetime curvature) in spacetime is determined by the nature of that curvature. Mathematically, the curvature of spacetime is determined by the Einstein equation, a central equation whose role in general relativity is equivalent to Newton's law of universal gravitation in classical mechanics and Maxwell's equations in electrodynamics:

$$G_{\alpha\beta} = 8\pi G T_{\alpha\beta}, \tag{1}$$

where G is Newton's universal gravitational constant. From here onwards, we will use geometrized units, wherein $G = c = 1$. (1) now reduces to:

$$G_{\alpha\beta} = 8\pi T_{\alpha\beta} \tag{2}$$

The right hand side of (2) contains the second rank tensor $T_{\alpha\beta}$, referred to as the stress energy tensor, which is a mathematical expression of the matter-energy source. $T_{\alpha\beta}$ is a 4×4 matrix with sixteen components. Written with upper indices, it takes the following form:

$$T^{\alpha\beta} = \begin{pmatrix} T^{tt} & T^{tx} & T^{ty} & T^{tz} \\ T^{xt} & T^{xx} & T^{xy} & T^{xz} \\ T^{yt} & T^{yx} & T^{yy} & T^{yz} \\ T^{zt} & T^{zx} & T^{zy} & T^{zz} \end{pmatrix} \tag{3}$$

(Note that upper and lower indices represent different quantities. In particular, $T_{\alpha\beta} = g_{\alpha\delta} g_{\beta\gamma} T^{\gamma\delta}$ with γ and δ summed over from 0 to 3; 0 represents the time coordinate and the rest, space coordinates; $g_{\alpha\beta}$ is a tensor quantity whose physical meaning will soon be explained.)

To give a more physical interpretation of the stress energy tensor, it is useful to look at it as a combination of a scalar that represents energy density, a row three-vector that represents intensity (energy per unit area per unit time), a column three-vector that represents momentum density (momentum per unit volume) and a 3×3 matrix whose components represent stresses (force per unit area).

$$T^{tt} \rightarrow \text{Energy Density} \quad \begin{pmatrix} T^{xx} & T^{xy} & T^{xz} \\ T^{yx} & T^{yy} & T^{yz} \\ T^{zx} & T^{zy} & T^{zz} \end{pmatrix} \rightarrow \text{Stress} \tag{4}$$

$$\begin{pmatrix} T^{tx} & T^{ty} & T^{tz} \end{pmatrix} \rightarrow \text{Intensity} \quad \begin{pmatrix} T^{xt} \\ T^{yt} \\ T^{zt} \end{pmatrix} \rightarrow \text{Momentum Density} \tag{5}$$

The left hand side of (2) contains the Einstein tensor $G_{\alpha\beta}$, which is a measure of the spacetime curvature caused by $T_{\alpha\beta}$. $G_{\alpha\beta}$ may be expressed in terms of the metric tensor $g_{\alpha\beta}$, which, as we shall soon see, is the central quantity that determines the trajectories of test particles. Therefore, solving the Einstein equation (2) yields the metric tensor $g_{\alpha\beta}$.

In four dimensional spacetime, the position four-vector is denoted as $\mathbf{x}$, or, in component form, as:

$$x^{\alpha} \equiv (x^0, x^1, x^2, x^3) \tag{6}$$

where x^0 is the time component and x^i, $i = 1, 2, 3$, are the space components. The distance between two infinitesimally separated points in spacetime is expressed in terms of the metric as:

$$ds^2 = g_{\alpha\beta} dx^{\alpha} dx^{\beta} \tag{7}$$

where, according to the Einstein summation convention, consecutive lower and upper greek indices are to be summed over from 0 to 3.

The trajectory of a particle betweem two points in curved spacetime is the equivalent of a straight line connecting two points in 3-dimensional Eucledian space. These "straight lines" in curved spacetime are referred to as "geodesics".

What we now need is a "geodesic equation" whose solution yields the geodesic followed by the particle in a given spacetime represented by the metric. This requires us to introduce a new quantity called the "proper time", denoted by τ and defined as:

$$d\tau^2 \equiv -ds^2 = -g_{\alpha\beta}dx^\alpha dx^\beta \tag{8}$$

Physically, the proper time represents the time measured by an observer moving along with the particle. The geodesic equation is found by extremizing the proper time between two coordinate points (say A and B) in spacetime.

$$\delta\tau_{AB} = 0 \Rightarrow \delta\int_A^B [-g_{\alpha\beta}dx^\alpha dx^\beta]^{1/2} = 0 \tag{9}$$

Using the calculus of variations, (9) yields the following equation in terms of τ:

$$\frac{d^2x^\alpha}{d\tau^2} = -\Gamma^\alpha_{\beta\gamma}\frac{dx^\beta}{d\tau}\frac{dx^\gamma}{d\tau} \tag{10}$$

where $\Gamma^\alpha_{\beta\gamma}$ are the so-called "Christoffel symbols" or "connection coefficients", and are built up from the metric $g_{\alpha\beta}$ as follows:

$$g_{\alpha\delta}\Gamma^\delta_{\beta\gamma} = \frac{1}{2}\left(\frac{\partial g_{\alpha\beta}}{\partial x^\gamma} + \frac{\partial g_{\alpha\gamma}}{\partial x^\beta} - \frac{\partial g_{\beta\gamma}}{\partial x^\alpha}\right) \tag{11}$$

Thus, (10) determines the trajectory of a particle in a spacetime described by the metric $g_{\alpha\beta}$, and plays a role similar to the second law equation in Newtonian mechanics.

2.2 The Kerr Metric

Using the Einstein equation (2), the spacetime (expressed in terms of the line element) around a spinning black hole with mass M and angular momentum J was predicted by Roy Kerr in 1963 to be:

$$\begin{aligned} ds^2_{Kerr} = \quad &- \quad \left(1 - \frac{2Mr}{\rho^2}\right)dt^2 - \frac{4MAr\sin^2\theta}{\rho^2}d\phi dt + \frac{\rho^2}{\Delta}dr^2 + \rho^2 d\theta^2 \\ &+ \quad \left(r^2 + A^2 + \frac{2MrA^2\sin^2\theta}{\rho^2}\right)\sin^2\theta d\phi^2 \end{aligned} \tag{12}$$

where $A \equiv aM$, $a \equiv J/M^2$, $\rho^2 = r^2 + A^2\cos^2\theta$, $\Delta \equiv r^2 - 2Mr + A^2$. The coordinates (t,r,$\theta$,$\phi$) are referred to as the "Boyer-Lindquist" coordinates, and "a" is the Kerr paramter, which is a measure of the spin of the black hole. The Kerr parameter is positive and cannot exceed 1, i.e, $0 \leq a \leq 1$.

The Kerr metric has several interesting properties. Those directly relevant to this thesis are listed below:

1) The metric (12) is asymptotically flat. This is expressed symbollically as:

$$R >> M,\ R >> A \Rightarrow ds^2_{Kerr} \rightarrow ds^2_{flat}, \tag{13}$$

where ds^2_{flat} is the line element for flat spacetime encountered in special relativity expressed in spherical polar coordinates:

$$ds^2_{flat} = -dt^2 + dr^2 + r^2 d\theta^2 + r^2 \sin^2\theta d\phi^2 \tag{14}$$

2) The Kerr metric blows up when $\Delta = 0$. This singularity turns out to be a coordinate sigularity. A coordinate singularity is a singularity that occurs because of the nature of the coordinate system, and not because something is physically breaking down. By appropriate coordinate transformation, this singularity disappears. There are two radii at which Δ vanishes:

$$\Delta = 0 \Rightarrow r = r_\pm = M \pm \sqrt{M^2 - A^2} \tag{15}$$

r_+ is referred to as the "outer event horizon radius" (or simply "event horizon radius"). Nothing, not even light, can escape from locations within this radius. Thus, information about all events occuring at radii smaller than $r = r_+$ can never reach infinity, hence the name "event horizon". Only radii greater than r_+ are astrophysically relevant and the thesis will concern itself with orbits outside the event horizon.

3) A special case of the Kerr black hole is the spherically symmetric non-rotating ($a = 0$) black hole known as the Schwarzschild black hole. The line element for the spacetime around a Schwarzschild black hole ($ds^2_{Schwarz}$) can be found from ds^2_{Kerr} by plugging $a = 0$. The result is given below:

$$ds^2_{Schwarz} = -\left(1 - \frac{2M}{r}\right) dt^2 + \left(1 - \frac{2M}{r}\right)^{-1} dr^2 + r^2 \left(d\theta^2 + \sin^2\theta d\phi^2\right) \tag{16}$$

The event horizon radius for the Schwarzschild black hole is $r_{hor} = 2M$, the radius at which the metric element $g_{rr} = 1/(1 - 2M/r)$ blows up.

2.3 Circular Equatorial Orbits

Equatorial orbits ($\theta = \pi/2$) are the easiest to handle mathematically. The Kerr line element for such orbits reduces to:

$$ds^2 = -\left(1 - \frac{2M}{r}\right) dt^2 - \frac{4AM}{r} dt d\phi + \frac{r^2}{\Delta} dr^2 + \left(r^2 + A^2 + \frac{2MA^2}{r}\right) d\phi^2 \tag{17}$$

The metric is independant of t and ϕ. The resulting symmetries generate two conserved quantities that

can be indentified as energy per unit rest mass e and angular momentum per unit rest mass l. The geodesic equations (10) may be expressed in terms of these conserved quantities, giving us the following equations of motion:

$$\begin{aligned}\frac{dt}{d\tau} &= \frac{1}{\Delta}\left[\left(r^2 + A^2 + \frac{2MA^2}{r}\right)e - \frac{2MA}{r}l\right] \\ \frac{d\phi}{d\tau} &= \frac{1}{\Delta}\left[\left(1 - \frac{2M}{r}\right)l + \frac{2MA}{r}e\right] \\ \frac{e^2-1}{2} &= \frac{1}{2}\left(\frac{dr}{d\tau}\right)^2 + V_{eff}(r,e,l)\end{aligned} \tag{18}$$

where

$$V_{eff}(r,e,l) = -\frac{M}{r} + \frac{l^2 - A^2(e^2-1)}{2r^2} - \frac{M(l-Ae)^2}{r^3} \tag{19}$$

is the effective potential for equatorial orbits. Just like in Newtonian gravity, V_{eff} contains information about the shape of the orbits.

Our thesis will focus largely on stable circular orbits. For these orbits, the radial velocity vanishes:

$$r = R = const \Rightarrow \frac{dr}{d\tau} = 0 \Rightarrow \frac{e^2-1}{2} = V_{eff}(R,e,l), \tag{20}$$

and the effective potential is a minimum:

$$\left[\frac{\partial V_{eff}}{\partial r}\right]_{r=R} = 0 \tag{21}$$

$$\left[\frac{\partial^2 V_{eff}}{\partial r^2}\right]_{r=R} > 0 \tag{22}$$

(From here onwards, for circular orbits, the constant orbital radius will be denoted as R and the event horizon radius as R_+. For general orbits, r and r_+ will still be used)

There is a limiting radius called the "Innermost Stable Circular Orbit Radius", or simply "ISCO Radius (R_{ISCO})" for short, below which no stable circular orbit can exist. This radius is found by turning inequality (22) to an equality and solving it along with equations (20) and (21) as a set of simultaneous equations for e, l and R. Eliminating e and l, we are left with the following quartic equation [17]:

$$1 - 6V^2 + 8aV^3 - 3a^2V^4 = 0, \tag{23}$$

where $V(R) = \sqrt{\frac{M}{R}}$ is a velocity parameter. Solving (23) yields the velocity parameter at the ISCO V_{ISCO}, and thus the ISCO radius R_{ISCO}. Fig: 1 shows the position of the ISCO with respect to the event horizon.

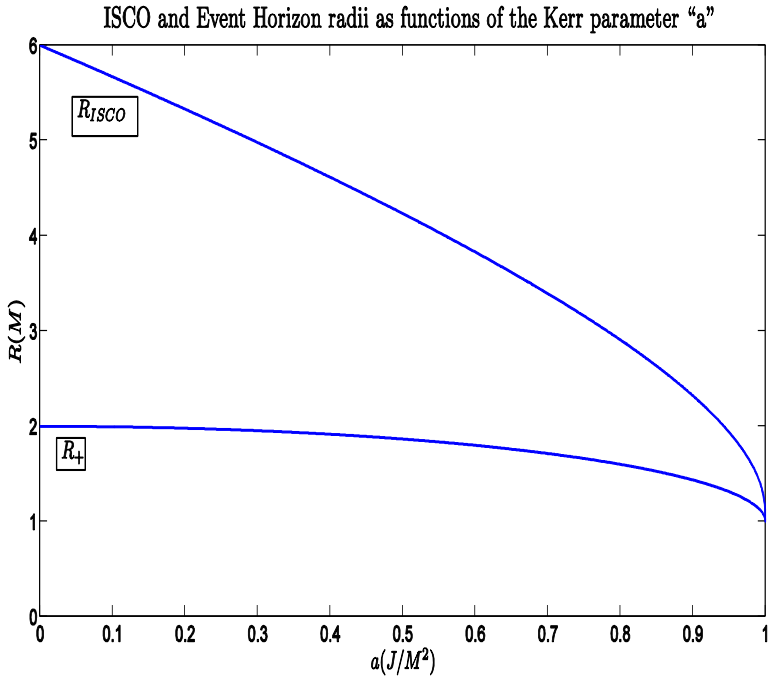

Figure 1: The ISCO radius varies from $R = 6M$ for a non-rotating/Schwarzschild black hole ($a = 0$) to $R = M$ for an extremally spinning black hole ($a = 1$), where it equals the event horizon radius.

2.4 Angular velocity of Horizon and Orbit

As mentioned in Section 1.3, the event horizon may be looked at as a physically viscous membrane that distorts under the influence of an external mass. The resulting bulges rotate with an angular velocity equal to that of the black hole, which is given by:

$$\Omega_H = \frac{a}{2R_+} \tag{24}$$

The angular velocity of the orbiting particle (as viewed by an observer far away from the black hole) is $\Omega_O = d\phi/dt = (d\phi/d\tau)/(dt/d\tau)$. For a given radius greater than R_{ISCO}, equations (20) and (21) may be solved simultaneously for e and l. These values of e and l may then be plugged into the expressions for $d\phi/d\tau$ and $dt/d\tau$ to calculate Ω_O (cf (18)). The result is given below [25]:

$$\Omega_O = \frac{M^{1/2}}{r^{3/2} + aM^{3/2}} \tag{25}$$

These angular velocities will be used in a later section to provide striking evidence for the equivalence between tidal friction and superradiant scattering talked about in the previous section.

3 Superradiant Scattering

(The term flux is often used to describe intensity, or energy per unit area per unit time. However, from this section onwards, as is commonly done in relativistic astrophysics, flux will be used to describe energy per unit time.)

3.1 The Teukolsky Formalism

To give a mathematical description of superradiant scattering, we need to solve the two body problem in general. But, unlike in Newtonian gravity where the two body problem is solvable analytically, the two body problem in general relativity has no known solution. However, the problem may be solved perturbatively in the extreme mass ratio case, where a particle of mass m orbits a black hole of mass M, with $m << M$. The approach that we will adopt is called the Teukolsky formalism.

The Teukolsky formalism assumes the particle to be the matter-energy source which causes a perturbation in the Kerr spacetime [19]. The latter is expressed in terms of the perturbed Weyl tensor $C_{\alpha\beta\gamma\delta}$. The Weyl tensor "[...] is equal to the Riemann tensor in vacuum" [10], and the Riemann tensor is a mathematical expression for the curvature of the four dimensional spacetime which is constructed from the Christoffel symbols and the metric (cf Section 2.1). The formalism then projects this tensor onto the Newman-Penrose tetrad, which is a set of four null unit spacetime vectors $l, n, m, \bar{m}$ (overbar represents complex conjugation) with the following orthogonality relationships [10]:

$$\begin{aligned} &\mathbf{l}\cdot\mathbf{l} = \mathbf{n}\cdot\mathbf{n} = \mathbf{m}\cdot\mathbf{m} = \bar{\mathbf{m}}\cdot\bar{\mathbf{m}} = 0 \\ &\mathbf{l}\cdot\mathbf{n} = 1; \mathbf{m}\cdot\bar{\mathbf{m}} = -1 \end{aligned} \tag{26}$$

The projection yields a scalar called the Weyl scalar $\psi_4 = -C_{\alpha\beta\gamma\delta}n^\alpha\bar{m}^\beta n^\gamma\bar{m}^\beta$, where [10]

$$\begin{aligned} n^\alpha &= \tfrac{1}{2\Sigma}\left(\left(r^2+A^2\right), -\Delta, 0, A\right), \\ m^\alpha &= \tfrac{1}{\sqrt{2}(r+iA\cos\theta)}\left(iA\cos\theta, 0, 1, i/\sin\theta\right) \end{aligned} \tag{27}$$

The central equation of the Teukolsky formalism is the differential equation for ψ_4 [10],

$$\begin{aligned} &\left[\frac{\left(r^2+A^2\right)^2}{\Delta} - A^2\sin^2\theta\right]\psi_{,tt} + \tfrac{4MAr}{\Delta}\psi_{,t\phi} + \left[\tfrac{A^2}{\Delta} - \tfrac{1}{\sin^2\theta}\right]\psi_{,\phi\phi} - \Delta^{-s}\left(\Delta^{s+1}\psi_{,r}\right)_{,r} \\ &-\tfrac{1}{\sin\theta}\left(\sin\theta\psi_{,\theta}\right)_{,\theta} - 2s\left[\tfrac{A(r-M}{\Delta} + \tfrac{i\cos\theta}{\sin^2\theta}\right]\psi_{,\phi} - 2s\left[\tfrac{M(r^2-A^2)}{\Delta} - r - iA\cos\theta\right]\psi_{,t} \\ &+(s^2\cot^2\theta - s)\psi = 4\pi\Sigma T \end{aligned} \tag{28}$$

where $\Delta = r^2 - 2Mr + A^2$, $\Sigma = r^2 + (A\cos\theta)^2$, $s = -2$, $\psi = \rho^{-4}\psi_4$, $\rho = 1/(r - iA\cos\theta)$, T is the source term, and a comma denotes partial differentiation.

T is a scalar found by projecting the stress-energy tensor of the perturbing source on to the Newman-Penrose tetrad. For a point particle with mass m in an arbitrary orbit around the Kerr black hole, the stress energy tensor is [12]:

$$T^{\alpha\beta} = m\frac{u^\alpha u^\beta}{\Sigma sin\theta u^t}\delta(r - r(t))\delta(\theta - \theta(t))\delta(\phi - \phi(t)) \tag{29}$$

where $u^\alpha = (dx^\alpha)/d\tau$ is the four-velocity of the particle.

ψ_4 contains all the information about gravitational waves travelling towards infinity and the horizon. From these waves, the energy flux emitted by the orbiting particle to infinity and the horizon may be calculated.

3.2 Calculating ψ

To solve the master perturbation equation (28), we first try to solve its corresponding homogeneous equation (i.e, set T = 0). By supposing [10]:

$$\psi = exp(-i\omega t)exp(im\phi)S(\theta)R(r), \tag{30}$$

(28) separates into a radial equation and an eigenvalue equation in $S(\theta)$. The radial equation is [18],[12]:

$$\left[\Delta^2\frac{d}{dr}\left(\frac{1}{\Delta}\frac{d}{dr}\right) - V(r)\right]R = 0 \tag{31}$$

with $V(r) = -\frac{K^2+4i(r-M)K}{\Delta} + 8i\omega r + \lambda$, $K = (r^2 + A^2) - mA$ and λ is an eigenvalue. The eigenvalue equation is [18],[12]:

$$\left[\frac{1}{\sin\theta}\left(\sin\theta\frac{d}{d\theta}\right) - A^2\omega^2\sin^2\theta + \frac{(m - 2\cos\theta)^2}{\sin^2\theta} + 4A\omega\cos\theta - 2 + 2mA\omega + \lambda\right]{}_{-2}S_{lm} = 0 \tag{32}$$

where λ is the eigenvalue of equation (32). Its eigenfuntions ${}_{-2}S_{lm}$ are the so called "spin weighted spheroidal harmonics" [12].

${}_{-2}S_{lm}$ are complete and orthogonal; we may then expand the source term in (28) using ${}_{-2}S_{lm}$ [10]:

$$4\pi\Sigma T = \int_{-\infty}^{\infty} d\omega\left[\sum_{l,m} exp(-i\omega t + im\phi){}_{-2}S_{lm}(\theta)T_{lm\omega}(r)\right] \tag{33}$$

Plugging (33) into (28), we find that the homogeneous radial equation turns into a nonhomogeneous

equation with $T_{lm\omega}(r)$ as source term on the right hand side of (31), while (32) remains unchanged. Denoting $R_{lm\omega}(r)$ as the solution to the inhomogeneous radial equation, ψ may finally be expressed as [10]:

$$\psi = \int_{-\infty}^{\infty} d\omega \left[\sum_{l,m} exp(-i\omega t + im\phi)_{-2}S_{lm}(\theta)R_{lm\omega}(r) \right] \tag{34}$$

3.3 Solving the Nonhomogeneous Radial Equation

The nonhomogeneous radial equation:

$$\left[\Delta^2 \frac{d}{dr}\left(\frac{1}{\Delta}\frac{d}{dr}\right) - V(r) \right] R_{lm\omega} = T_{lm\omega} \tag{35}$$

contains the energy flux information we are seeking to determine.

The program for solving (35) requires the use of the Green's function technique, and goes as follows [20]:

1) We construct the corresponding homogeneous equation by setting $T_{lm\omega} = 0$, which is simply (31).

2) The range of interest for r is $]r_+, \infty[$, i.e, the region between the event horizon and infinity. We expect (31), which is a second order differential equation, to have two linearly independant solutions R^{in} and R^{out}. R^{in} satisfies the boundary condition at $r \to r_+$ and R^{out} satisfies the boundary condition at $r \to \infty$.

3) We determine the two asymptotic equations of (31): one when $r \to \infty$ (far away from BH), the other when $r \to r_+$ (at event horizon of BH), and solve for R.

4) The boundary conditions on (35) apply to (31) as well. Using these boundary conditions, we may determine the solutions of the asymptotic equations, viz. R_∞ and R_{r_+}.

5) The Green's function has the following form:

$$G(r,r') = \begin{cases} G^{in}(r,r') & \text{for } r_+ < r < r' \\ G^{out}(r,r') & \text{for } r' < r < \infty \end{cases} \tag{36}$$

G^{in} and G^{out} are constructed from R^{in} and R^{out}, their asymptotic forms, and their Wronskian.

6)The nonhomogeneous equation is of the form $\mathcal{L}R_{lm\omega}(r') + f(r') = 0$, and the homogeneous equation is of the form $\mathcal{L}R(r') = 0$, where $\mathcal{L} = \frac{d}{dr'}\left(p(r')\frac{d}{dr'}\right) + q(r')$ is the self adjoint operator. Assuming R^{in} and R^{out} to be linearly independant, the Wronskian $W(r')$ must equal $Q/p(r')$, where Q is a constant. Explicitly:

$$R^{in}(r')\frac{dR^{out}(r')}{dr'} - R^{out}(r')\frac{dR^{in}(r')}{dr'} = \frac{Q}{p(r')} \tag{37}$$

$$\Rightarrow Q = p(r')\left[R^{in}(r')\frac{dR^{out}(r')}{dr'} - R^{out}(r')\frac{dR^{in}(r')}{dr'} \right] \tag{38}$$

We can now determine the Green's function for (31):

$$G(r,r') = \begin{cases} G^{in}(r,r') = -\frac{R^{in}(r)R^{out}(r')}{Q} & \text{for } r_+ < r < r' \\ G^{out}(r,r') = -\frac{R^{in}(r')R^{out}(r)}{Q} & \text{for } r' < r < \infty \end{cases} \tag{39}$$

Using the symmetry of $G(r,r')$, viz. $G(r,r') = G(r,r')$, we find that:

$$G(r,r') = \begin{cases} G^{out}(r,r') = -\frac{R^{in}(r')R^{out}(r)}{Q} & \text{for } r_+ < r' < r \\ G^{in}(r,r') = -\frac{R^{in}(r)R^{out}(r')}{Q} & \text{for } r < r' < \infty \end{cases} \tag{40}$$

7) Finally, $R_{lm\omega}$ is evaluated using the source term and Green's funtion:

$$\begin{aligned} R_{lm\omega} &= \int_{r_+}^{\infty} G(r,r')f(r')dr' \\ &= \int_{r_+}^{r} G^{out}(r,r')f(r')dr' + \int_{r}^{\infty} G^{in}(r,r')f(r')dr' \end{aligned} \tag{41}$$

3.4 Asymtpotic Forms of the Homogeneous Radial Equation

The nonhomogeneous radial equation may be written as:

$$\left[\frac{d}{dr}\left(\frac{1}{\Delta}\frac{d}{dr}\right) - \frac{V(r)}{\Delta^2}\right] R_{lm\omega} = \frac{T_{lm\omega}}{\Delta^2} \tag{42}$$

The homogeneous radial equation is therefore:

$$\left[\frac{d}{dr}\left(\frac{1}{\Delta}\frac{d}{dr}\right) - \frac{V(r)}{\Delta^2}\right] R = 0 \tag{43}$$

Defining new variables $Y = \Delta^{-1}(r^2+A^2)^{1/2}R$ and $\frac{dr*}{dr} = \frac{(r^2+A^2)}{\Delta}$, the homogeneous equation's asymptotic forms and their solutions are found to be [10]:

$$r \to \infty \begin{cases} \frac{d^2Y}{dr_*^2} + \left(\omega^2 - \frac{4i\omega}{r}\right) Y = 0 \\ \Rightarrow Y \sim r^{\pm 2} exp(\pm i\omega r_*) \\ \Rightarrow R \sim \frac{exp(-i\omega r_*)}{r} \equiv R_{\infty 1}; R \sim r^3 exp(i\omega r_*) \equiv R_{\infty 2} \\ \Rightarrow R_\infty = B^{in}R_{\infty 1} + B^{out}R_{\infty 2} \end{cases} \tag{44}$$

$$r \to r_+ \begin{cases} \frac{d^2Y}{dr_*^2} + \left[k^2 + 4i(r_+ - M)\frac{k}{2Mr_+} - \frac{r_+ - M}{(Mr_+)^2}\right] Y = 0 \\ \Rightarrow Y \sim \Delta^{\pm 1} exp(\mp ikr_*) \\ \Rightarrow R \sim exp(ikr_*) \equiv R_{r_+2}; R \sim \Delta^2 exp(-ikr_*) \equiv R_{r_+1} \\ \Rightarrow R_{r_+} = C^{in}R_{r_+1} + C^{out}R_{r_+2} \end{cases} \tag{45}$$

Here, $k = \omega - m\omega_+$ and $\omega_+ = a/(2r_+)$.

3.5 Constructing the Asymptotic Solutions of the Homogeneous Equation

The boundary conditions on (35) require the gravitational waves at infinity to be purely outgoing, since no waves are expected to be reflected from infinity. (Note that we are assuming the black hole-particle system to be isolated). Since R^{out} needs to satisfy this boundary condition, $R^{out}(r \to \infty) = R_{\infty 2} = r^3 exp(i\omega r_*)$. The waves at the horizon are expected to be purely ingoing. Since R^{in} needs to satisfy this boundary condition, $R^{in}(r \to r_+) = R_{r_+1} = \Delta^2 exp(-ikr_*)$. The boundary conditions impose no restriction on the asymptotic form of R^{in} at infinity and R^{out} at the horizon. Therefore, $R^{in}(r \to \infty) = R_\infty$. By a similar argument, $R^{out}(r \to r_+) = R_{r_+}$. Thus [12]:

$$R^{out} \begin{cases} R^{out}(r \to r_+) = C^{in}\Delta^2 exp(-ikr_*) + C^{out} exp(ikr_*) \\ R^{out}(r \to \infty) = r^3 exp(i\omega r_*) \end{cases} \tag{46}$$

$$R^{in} \begin{cases} R^{in}(r \to \infty) = B^{in}\frac{exp(-i\omega r_*)}{r} + B^{out} r^3 exp(i\omega r_*) \\ R^{in}(r \to r_+) = \Delta^2 exp(-ikr_*) \end{cases} \tag{47}$$

3.6 Determining $R_{lm\omega}$

We are now in a position to determine the constant Q (cf Eq (38)). Identifying $p = 1/\Delta^2$, and using equation (38), we determine the constant Q. Since Q is independant of r', we can use the forms of R^{in} and R^{out} at infinity to determine Q. Explicitly:

$$\begin{aligned} lim_{r' \to \infty} Q &= lim_{r' \to \infty} p(r') \left[R^{in}(r') \frac{dR^{out}(r')}{dr'} - R^{out}(r') \frac{dR^{in}(r')}{dr'} \right] \\ &= lim_{r' \to \infty} p(r') \left[R_\infty(r') \frac{dR_{\infty 2}(r')}{dr'} - R_{\infty 2}(r') \frac{dR_\infty(r')}{dr'} \right] \\ &= 2i\omega B^{in} \end{aligned} \tag{48}$$

Then (cf. (39)):

$$G(r, r') = \begin{cases} G^{out}(r, r') = -\frac{R^{in}(r')R^{out}(r)}{2i\omega B^{in}} & \text{for } r_+ < r' < r \\ G^{in}(r, r') = -\frac{R^{in}(r)R^{out}(r')}{2i\omega B^{in}} & \text{for } r < r' < \infty \end{cases} \tag{49}$$

Identifying $f(r') = T_{lm\omega}/\Delta^2$, $R_{lm\omega}$ may finally be determined (cf: (41)) [12]:

$$\begin{aligned} R_{lm\omega} &= \int_{r_+}^{\infty} G(r,r')f(r')dr' \\ &= \frac{R^{out}(r)}{2i\omega B^{in}} \int_{r_+}^{r} \frac{T_{lm\omega}(r')R^{in}(r')}{\Delta^2(r')}dr' + \frac{R^{in}(r)}{2i\omega B^{in}} \int_{r}^{\infty} \frac{T_{lm\omega}(r')R^{out}(r')}{\Delta^2(r')}dr' \end{aligned} \tag{50}$$

3.7 Energy Flux at Infinity and the Horizon

We seek to determine the energy flux associated with the gravitational waves going to infinity and the horizon. Clearly, then, what we need to to focus on is $R_{lm\omega}(r \to \infty)$ and $R_{lm\omega}(r \to r_+)$. It is clear from equations (50), (46), (47) [12]:

$$R_{lm\omega}(r \to r_+) = \frac{\Delta^2 exp(-ikr_*)}{2i\omega B^{in}} \int_{r_+}^{\infty} \frac{T_{lm\omega}(r')R^{out}(r')}{\Delta^2(r')}dr' \equiv Z^{\infty}_{lm\omega}\Delta^2(r)exp(-ikr_*) \tag{51}$$

$$R_{lm\omega}(r \to \infty) = \frac{r^3 exp(i\omega r_*)}{2i\omega B^{in}} \int_{r_+}^{\infty} \frac{T_{lm\omega}(r')R^{in}(r')}{\Delta^2(r')}dr' \equiv Z^{H}_{lm\omega}r^3 exp(i\omega r_*) \tag{52}$$

We now need to establish a connection between the Z amplitudes and the energy flux. To do that, we first need to introduce a quantitative way to express the energy carried by gravitational waves [21].

3.8 Relating the Z amplitudes to the Energy Flux

(Note that in this subsection, unless otherwise specified, the equations are standard equations in general relativity, and have been taken from J.Hartle's textbook titled "Gravity" [21])

The Kerr metric is asymptotically flat. Therefore, the gravitational waves at infinity may be looked at as perturbations of the flat spacetime metric:

$$g_{\alpha\beta} = \eta_{\alpha\beta}(\text{flat}) + \text{h}_{\alpha\beta}(\text{perturbation}) \tag{53}$$

The Einstein equation may then be expanded to first order in $h_{\alpha\beta}$, and the resulting equation has two linearly independant solutions. A linear combination of these solutions also solves the Einstein equation expanded to first order. This is a property of these so-called linearized solutions. The full non-linear Einstein equation and their solutions do not in general have this property.

With appropriate choice of coordinates, these solutions can be viewed as two independant transverse polarizations. To get a feel for what these polarizations are, we may picture the effect of a gravitational wave on a circular ring of test masses situated in a plane perpendicular to the direction of propagation (z direction). The gravitational waves incident on the ring will cause one of the axes (lets call it x) to elongate

and the other to contract (lets call it y), distorting the circle into a horizontal ellipse. The length of these axes continually oscillate out of phase, thus periodically changing the shape of the ring from horizontal to vertical ellipses. Mathematically, this polarization (referred to as the "plus" polarization) is expressed as:

$$h_{\alpha\beta}(t,z) = \begin{pmatrix} 0 & 0 & 0 & 0 \\ 0 & 1 & 0 & 0 \\ 0 & 0 & -1 & 0 \\ 0 & 0 & 0 & 0 \end{pmatrix} h_+(t-z) \tag{54}$$

where h_+ represents the amplitude of the plus polarized wave.

The other polarization (referred to as the "cross" polarization) is found by rotating the $x-y$ axes by $\pi/4$. The behavior of the ring of masses is identical to that of the plus polarization, except the oscillating ellipse is rotated by $\pi/4$. Mathematically:

$$h_{\alpha\beta}(t,z) = \begin{pmatrix} 0 & 0 & 0 & 0 \\ 0 & 0 & 1 & 0 \\ 0 & 1 & 0 & 0 \\ 0 & 0 & 0 & 0 \end{pmatrix} h_\times(t-z) \tag{55}$$

where $h_\times$ represents the amplitude of the cross polarized wave. The general solution is a linear combination of both polarizations, viz:

$$h_{\alpha\beta} = h_+ + h_\times \tag{56}$$

There is a relationship that connects the energy flux at infinity and both polarizations of the perturbed metric h_+ and $h_\times$ [12]:

$$\left(\frac{dE}{dt}\right)^\infty = \frac{1}{16\pi}\int \left(h^2_{+,t} + h^2_{\times,t}\right) r^2 d\Omega \tag{57}$$

There is also a relationship that connects the Weyl scalar and the two polarizations [12]:

$$\psi_4 = \frac{1}{2}\left(h_{+,tt} - i h_{\times,tt}\right) \tag{58}$$

All the pieces are now in place to calculate the energy flux at infinity. We determine ψ_4 from the Teukolsky formalism, writing the result in terms of the Z amplitudes. We then use Eq (58) to relate ψ_4, and thus the Z amplitudes, to the perturbed metric (56). And finally, we use the flux formula (57) to calculate

energy flux in terms of the amplitudes Z.

The energy flux at the horizon proves to be far more complicated to calculate, since at the horizon, the Kerr spacetime is no longer asymptotically flat. Nonetheless, Teukolsky and Press [22] studied the distortion of the event horizon caused by impinging gravitational waves, in particular, the rate of change of the area of the event horizon, and related it to the energy flux down the hole. We just mention the final result here.

To quote the results, we first need to define two new variables, Z_{lmk} and ω_{mk}. The gravitational wave frequency is related to a combination of the harmonics of two orbital frequencies, Ω_r and Ω_ϕ. Ω_r is simply $2\pi/T_r$, where T_r is the period of the radial position function of the particle, $r(t)$, and $\Omega_\phi = \Delta\phi/T_r$, with $\Delta\phi = \phi(t+T_r) - \phi(t)$. Z_{lmk} are related to the gravitational wave frequencies via delta funcitons. Explicity [12],

$$\omega_{mk} = m\Omega_\phi + k\Omega_r \tag{59}$$

$$Z^{\infty,H}_{lm\omega} = \sum_{k=-\infty}^{+\infty} Z^{\infty,H}_{lmk}\,\delta(\omega - \omega_{mk}) \tag{60}$$

Using these variables, the flux at infinity is found to be [12]:

$$\left(\frac{dE}{dt}\right)^{\infty} = \sum_{l,m,k} \frac{|Z_{lmk}|^2}{4\pi\omega^2_{mk}} \tag{61}$$

Note that, as we would expect, the flux depends on the wave amplitudes Z and the wave frequencies ω_{mk}, which are themselves related to the orbital frequencies.

The expression for the flux at the horizon proves to be far more messy, and is quoted below [12]:

$$\left(\frac{dE}{dt}\right)^{H} = \sum_{l,m,k} \alpha_{lmk} \frac{|Z_{lmk}|^2}{4\pi\omega^2_{mk}} \tag{62}$$

where:

$$\alpha_{lmk} = \frac{256(2mr_+)^5 k(k^2+4\epsilon^2)(k^2+16\epsilon^2)\omega^3_{mk}}{C_{lmk}} \tag{63}$$

and

$$
\begin{aligned}
C_{lmk} = \quad & [\quad (\lambda+2)^2 + 4Am\omega_{mk} - 4A\omega_{mk}^2] \\
& \times \quad (\lambda^2 + 36Am\omega_{mk} - 36A^2\omega_{mk}^2) + (2\lambda+3)(96A^2\omega_{mk}^2) \\
& - \quad 48Am\omega_{mk}) + 144\omega_{mk}^2(M^2 - A^2)
\end{aligned} \tag{64}
$$

with $\epsilon = \sqrt{M^2 - A^2}/4Mr_+$.

3.9 Numerical Results for Equatorial Orbits

(Note that from this section onwards, for numerical calculations, we assume the smaller test mass to have a value $m = 10^3 M_\odot$ and the larger black hole to have a mass of to be $M = 10^9 M_\odot$, so that their ratio is $m/M = 10^{-6}$. We also define $L_H \equiv \left(\frac{dE}{dt}\right)^H$ and $L_\infty \equiv \left(\frac{dE}{dt}\right)^\infty$.)

The Z amplitudes may be determined numerically and the fluxes at infinity (L_∞) and the horizon (L_H) may be computed. In this section, we show results for circular ($r = R =$ constant) equatorial orbits . A negative L_H corresponds to the particle gaining orbital energy. This is what we earlier called superradiant scattering, and we shall hereafter refer to this flux as superradiant flux (L_S). Mathematically:

$$
L_S = \begin{cases} 0, \ L_H \geq 0 \\ L_H, \ L_H < 0 \end{cases}
$$

By varying the spin parameter a, we study its effect on L_H and, more crucially, on the ratio of the fluxes (i.e, L_H/L_∞). Fig: 2 is a plot of these fluxes.

Fig: 2 suggests two things:

1) $|L_S|$ increases with increasing black hole spin.

2) For all spins (i.e, $a = 0.1, 0.2, ...0.8, 0.9$ and 0.99), and for all radii outside the ISCO ($R_{ISCO} < R < 10M_\odot$), $|L_S| << L_\infty$. Fig: 3 shows this more clearly.

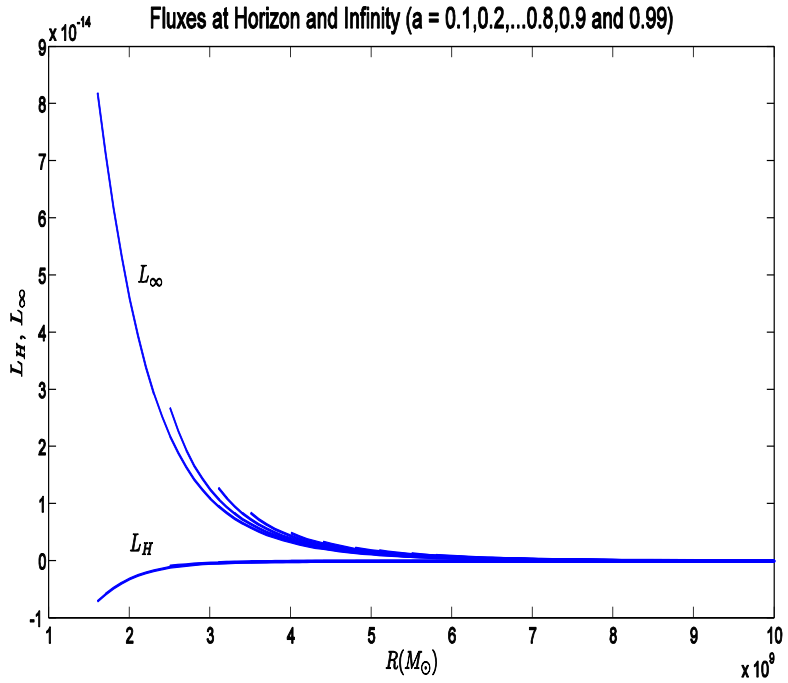

Figure 2: The spin parameter is varied from $a = 0$ to $a = 0.9$ in increments of $\Delta a = 0.1$. $a = 0.99$ is also included. The radius is varied from $R = 10M$ to $R = R_{ISCO}$ in decrements of $\Delta R = 0.1M$. It seems evident from the figure that, for all values of a used, $|L_H|$,$|L_S| << L_\infty$.

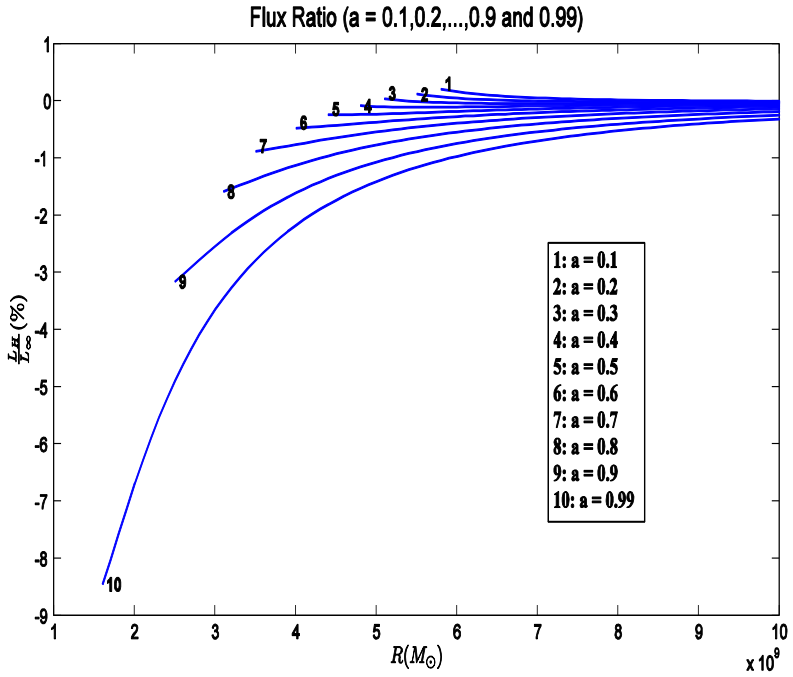

Figure 3: From the figure, $|L_S|$ is at best about 8% (for $a = 0.99$) of L_∞, which occurs when $a = 0.99$ and $R = R_{ISCO}$. For a floating orbit, we require a ratio of 100%.

The maximum value that a can take is unity. To estimate the maximum possible superradiant flux ratio (i.e, the maximum possible value of $|L_S|/L_\infty$), we require a plot of the maximum superradiant flux ratio (for each a) as a function of a, and, using a polynomial fit, extrapolate to the limiting Kerr parameter value of $a = 1$. The result is shown in Fig: 4

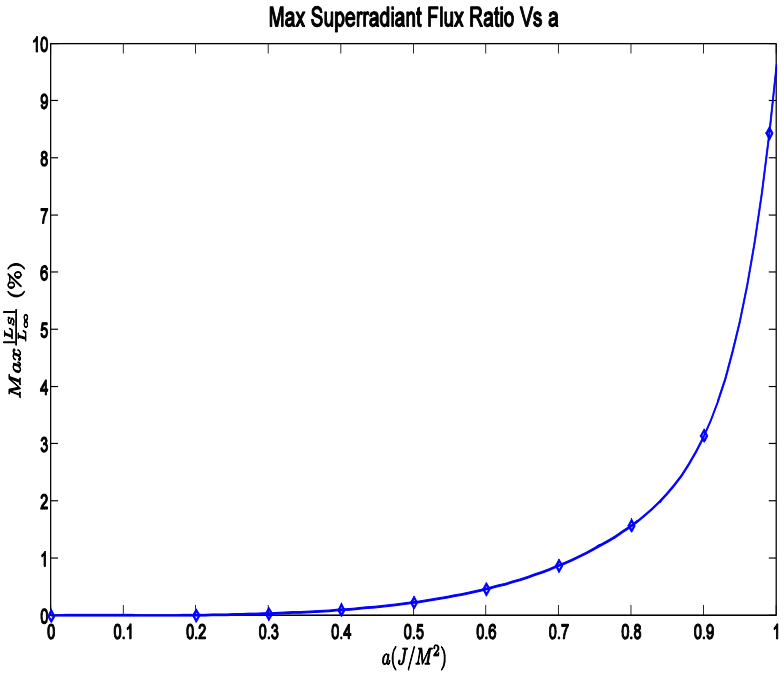

Figure 4: The extrapolated estimate (using a 12th degree polynomial fit) for the magnitude of the maximum possible superradiant flux ratio is close to 10%.

The maximum possible superradiant flux ratio for circular equatorial orbits is estimated to be 10%. For a floating orbit, this ratio needs to be 100%. Thus, superradiant scattering by itself cannot provide the necessary energy flux to allow a floating orbit. This result was previously found by Glampedakis and Kennefick [12].

Since the superradiant flux ratio for $a = 0.99$ and $a = 1$ differ by just about 1% , we will use $a = 0.99$ for future calculations that require maximum $|L_S|$.

3.10 A Note on the Transfer of Energy from Spin to Orbit

At this juncture, it is perhaps worth mentioning that the assumption that all of the black hole's lost spin energy is used to increase the orbiting body's orbital energy is not always true. If the body is a particle, as we have assumed so far, this assumption does hold. However, since the thesis focusses on binary black holes, the orbiting particle is in fact another non-spinning black hole whose mass is much smaller than the larger

black hole it is oribiting. In that event, not all the spin energy goes into orbital energy. From the first law of black hole mechanics [26]:

$$dM = \frac{k}{8\pi} dA + \Omega_H dJ + \Phi dQ \tag{65}$$

where dM is the change in mass-energy of the black hole, k is the surface gravity, dA the change in area of the event horizon, Ω_H the angular velocity of the event horizon, dJ the change in spin angular momentum, Φ the potential, and dQ the change in charge. This treatise deals with uncharged black holes, and therefore the first law, written as a time-rate equation, reduces to:

$$\frac{dM}{dt} = \frac{k}{8\pi} \frac{dA}{dt} + \Omega_H \frac{dJ}{dt} \tag{66}$$

$\Omega_H \frac{dJ}{dt}$ represents gain in spin energy, and $\frac{k}{8\pi} \frac{dA}{dt}$ represents energy used up to increase the black hole's event horizon area. From the second law of black hole mechanics [26]:

$$\frac{dA}{dt} \geq 0 \tag{67}$$

Therefore, not all the spin energy extracted by the smaller black hole is transferred to orbital energy. Some of it is "lost" to increasing the area of the event horizon. However, this fact does not in any way alter our results, since, even after assuming that all the spin energy is converted to orbital energy, the orbital energy lost to infinity far exceeds the energy gained from spin.

3.11 Support for the Equivalence of Superradiant Scattering and Tidal Friction

Using the data generated for studying superradiant scattering, we can give numerial support for the previously mentioned equivalence between superradiant scattering and tidal friction. As shown in Fig: 6, for $a = 0.4, 0.5, ..., 0.8, 0.9$ and 0.99, $L_H < 0$. Therefore, superradiant scattering, and correspondingly the transfer of black hole spin energy to orbital energy of the binary, occurs for these Kerr parameter values for radii outside the ISCO. For $a = 0.2$, $L_H < 0$ when $R > 7.27M = 7.27 \times 10^9 M_\odot$, and therefore superradiant scattering occurs from $R = 7.27M$ onwards. For $a = 0.3$, $L_H < 0$ when $R > 5.45M = 5.45 \times 10^9 M_\odot$, and therefore superradiant scattering occurs from $R = 5.45M$ onwards. For $a = 0.1$, $L_H > 0$ for the range of R plotted (i.e, $R_{ISCO} < R < 10M$).

In the tidal friction picture, the transfer of energy from the black hole's spin to the binary's orbit is closely connected with the magnitudes of the relative angular velocities of orbit (Ω_O) and spin (Ω_H). Thorne et al [14] and S. Hughes [15] encourage us to think about $\Omega_H > \Omega_O$ as a situation in which the bulge of the tidally

distorded event horizon of the black hole leads the orbiting particle, thereby exerting a torque that imparts its spin energy to the particle's orbital energy. In the superradiant scattering picture, this must correspond to $L_H < 0$, if the equivalence between tidal friction and superradiant scattering holds. Similarly, $\Omega_H < \Omega_O$ is a situation where the tidal bulge lags the particle, thus being torqued forward by the particle. Conversely, the particle is torqued backward by the bulge, thereby losing orbital energy to the black hole's spin energy. In the superradiant scattering picture, this must correspond to $L_H > 0$ for the equivalence to hold. And finally, $\Omega_H = \Omega_O$ is a situation where the bulge and the particle are corotating, and therefore, neither the bulge nor the particle is able to exert a torque on the other, resulting in no energy transfer between spin and orbit. In the superradiant scattering picture, this must correspond to $L_H = 0$. Thus, in summary, for the equivalence to hold:

$$\Omega_H > \Omega_O \Leftrightarrow L_H < 0 \tag{68}$$

$$\Omega_H < \Omega_O \Leftrightarrow L_H > 0 \tag{69}$$

$$\Omega_H = \Omega_O \Leftrightarrow L_H = 0 \tag{70}$$

Since $\Omega_O = \Omega_O(R, a)$ and $\Omega_H = \Omega_H(a)$ (cf Section 2.4), it should be possible to determine algebraicly the radii and Kerr parameters for which $\Omega_H > \Omega_O$, $\Omega_H < \Omega_O$ and $\Omega_H = \Omega_O$. From (25) and (24), (70) may be solved for R:

$$\Omega_H = \Omega_O \Rightarrow R = R_\Omega(a) \tag{71}$$

where

$$R_\Omega(a) = \left(\frac{2 - a^2 + 2\sqrt{1 - a^2}}{a} \right)^{2/3} M \tag{72}$$

It is now straightforward to show that:

$$R > R_\Omega \Rightarrow \Omega_H > \Omega_O \text{ and } \mathrm{R} < \mathrm{R}_\Omega \Rightarrow \Omega_\mathrm{H} < \Omega_\mathrm{O} \tag{73}$$

Fig: 5 shows clearly that when $a > 0.36$, $R_\Omega < R_{ISCO}$.

Since we are dealing with radii greater than the ISCO radius ($R > R_{ISCO}$), it follows that:

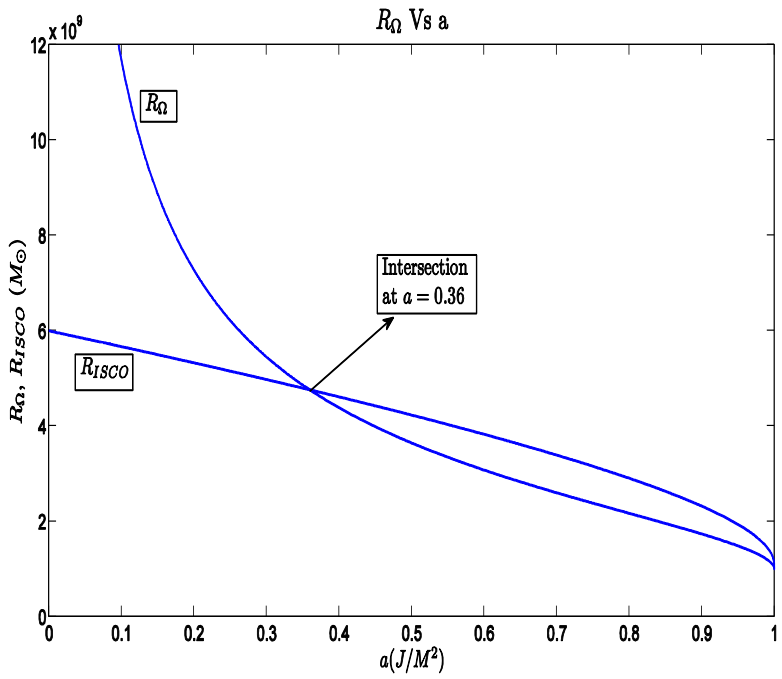

Figure 5: From the figure, it is clear that $R_\Omega < R_{ISCO}$ when $a > 0.36$. Thus, for $a > 0.36$, $\Omega_H > \Omega_O$ for all radii outside the ISCO.

$$a > 0.36 \Rightarrow R_\Omega < R_{ISCO} < R \tag{74}$$

Thus, from (73),

$$a > 0.36 \Rightarrow \Omega_H > \Omega_O \text{ for all R greater than } \mathrm{R_{ISCO}} \tag{75}$$

We had found from our results for superradiant scattering that $L_H < 0$ for $a = 0.4, 0.5, ..., 0.8, 0.9$ and 0.99, and $R > R_{ISCO}$ (cf Fig: 6). These Kerr parameters are all greater than 0.36. Clearly,

$$a > 0.36 \Rightarrow \Omega_H > \Omega_O \text{ and } \mathrm{L_H} < 0 \tag{76}$$

Thus (68) seems to hold, suggesting the equivalence between superradiant scattering and tidal friction.

For $a = 0.1$, $R_\Omega = 11.7M = 1.17 \times 10^9 M_\odot$. Therefore, $\Omega_H < \Omega_O$ for $R < 1.17 \times 10^9 M_\odot$. From our results for superradiant scattering, $L_H > 0$ for the range of R plotted, which is $R_{ISCO} < R < 10 \times 10^9 M_\odot$ (cf. Fig: 6b). Thus, (69) seems to hold, once again suggesting the equivalence between superradiant scattering scattering and tidal friction.

And finally, for $a = 0.2$ and $a = 0.3$, $R_\Omega = 7.27M = 7.27 \times 10^9 M_\odot$ and $R_\Omega = 5.45M = 5.45 \times 10^9 M_\odot$.

Thus:

$$a = 0.2 \rightarrow R = 7.27M \Rightarrow \Omega_H = \Omega_O \tag{77}$$

$$a = 0.3 \rightarrow R = 5.45M \Rightarrow \Omega_H = \Omega_O \tag{78}$$

and

$$a = 0.2 \rightarrow R > 7.27M \Rightarrow \Omega_H > \Omega_O \text{ and R} < 7.27\text{M } \Rightarrow \Omega_\text{H} < \Omega_\text{O} \tag{79}$$

$$a = 0.3 \rightarrow R > 5.45M \Rightarrow \Omega_H > \Omega_O \text{ and R} < 5.45\text{M } \Rightarrow \Omega_\text{H} < \Omega_\text{O} \tag{80}$$

From our results for superradiant scattering (cf: Fig: 6d, 6f):

$$a = 0.2 \rightarrow R = 7.27M \Rightarrow L_H = 0 \tag{81}$$

$$a = 0.3 \rightarrow R = 5.45M \Rightarrow L_H = 0 \tag{82}$$

and

$$a = 0.2 \rightarrow R > 7.27M \Rightarrow L_H < 0 \text{ and R} < 7.27\text{M } \Rightarrow \text{L}_\text{H} > 0 \tag{83}$$

$$a = 0.3 \rightarrow R > 5.45M \Rightarrow L_H < 0 \text{ and R} < 5.45\text{M } \Rightarrow \text{L}_\text{H} > 0 \tag{84}$$

Clearly, (68), (69), and (70) hold. This is perhaps the most striking evidence for the equivalence between superradiant scattering and tidal friction.

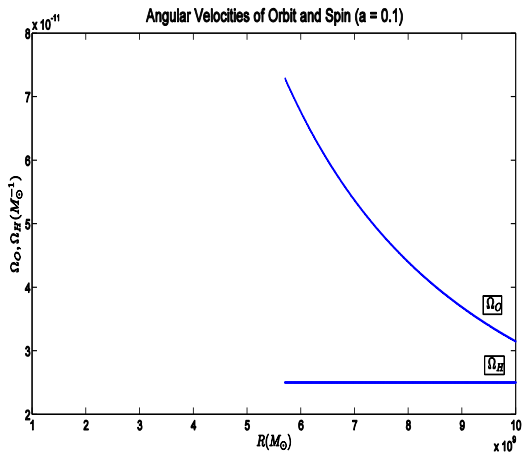

(a) When $R < 10M$, $\Omega_H < \Omega_O$

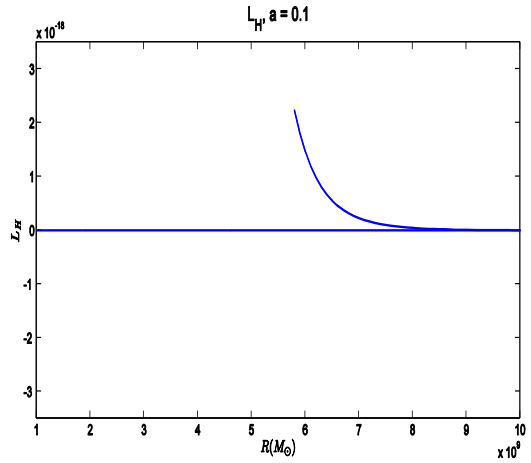

(b) When $R < 10M$, $L_H > 0 \Rightarrow$ No Superradiance

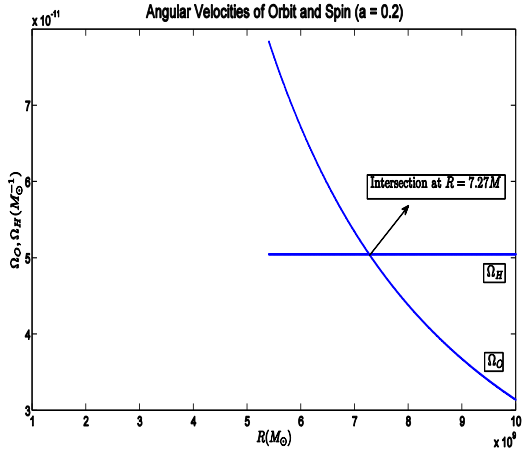

(c) When $R > 7.27M$, $\Omega_H > \Omega_O$

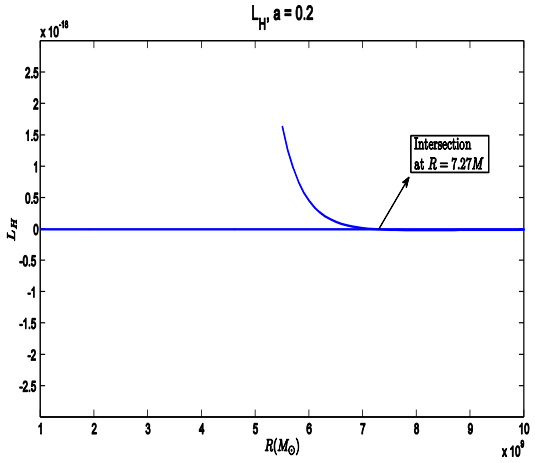

(d) When $R > 7.27M$, $L_H < 0 \Rightarrow$ Superradiance

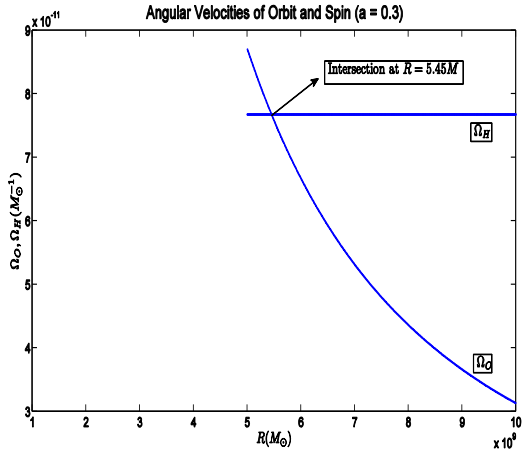

(e) When $R > 5.45M$, $\Omega_H > \Omega_O$

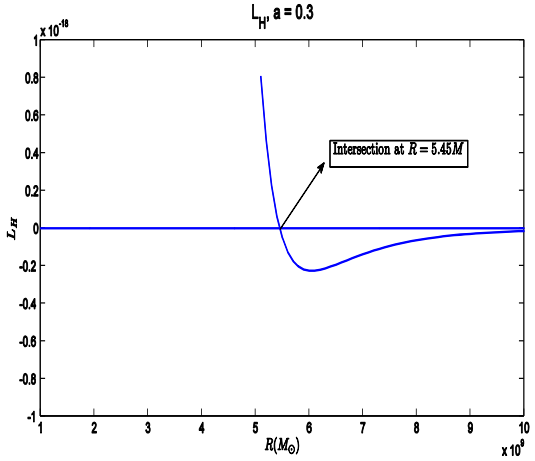

(f) When $R > 5.45M$, $L_H < 0 \Rightarrow$ Superradiance

Figure 6: Evidence for the equivalence between superradiant scattering and tidal friction.

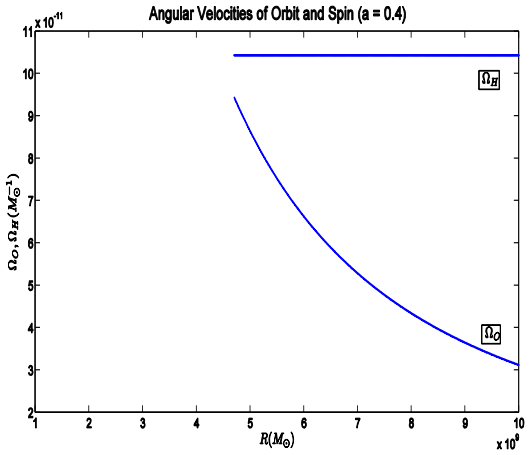

(g) When $R > R_{ISCO}$, $\Omega_H > \Omega_O$

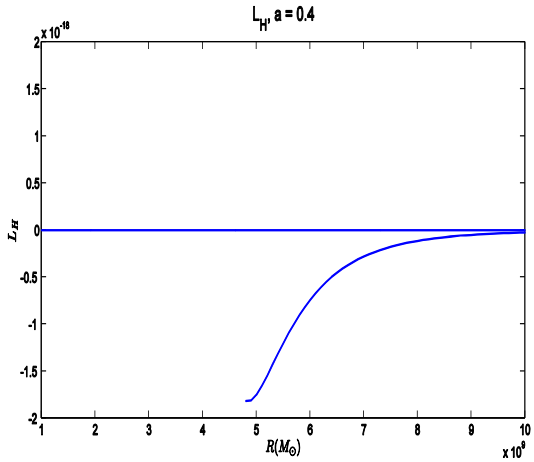

(h) When $R > R_{ISCO}$, $L_H < 0 \Rightarrow$ Superradiance

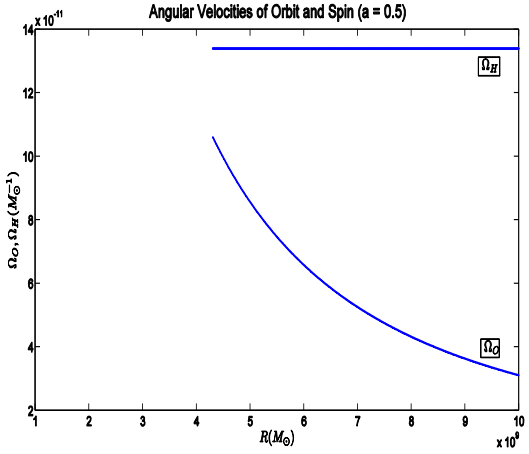

(i) When $R > R_{ISCO}$, $\Omega_H > \Omega_O$

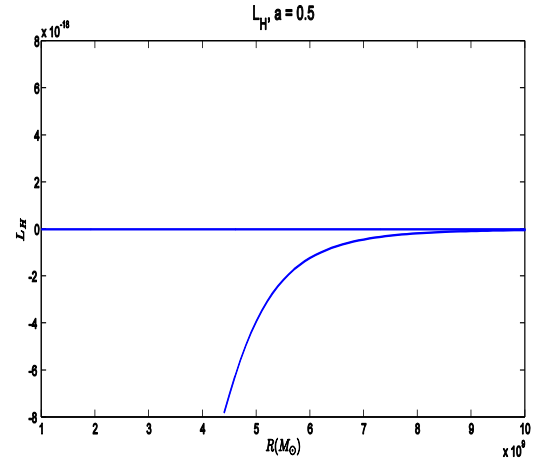

(j) When $R > R_{ISCO}$, $L_H < 0 \Rightarrow$ Superradiance

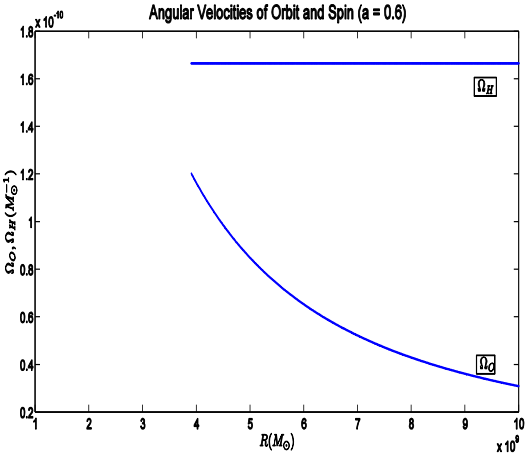

(k) When $R > R_{ISCO}$, $\Omega_H > \Omega_O$

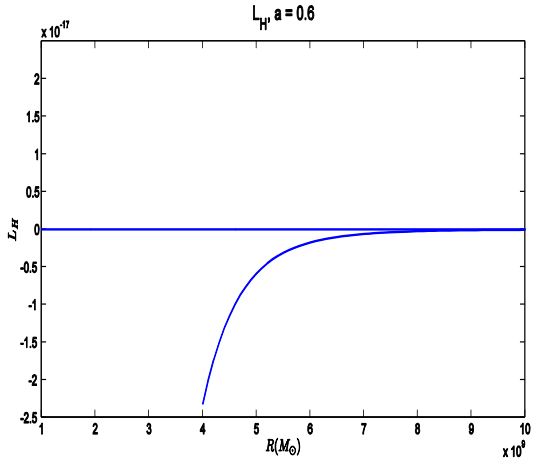

(l) When $R > R_{ISCO}$, $L_H < 0 \Rightarrow$ Superradiance

Figure 6: Evidence for the equivalence between superradiant scattering and tidal friction (cont.).

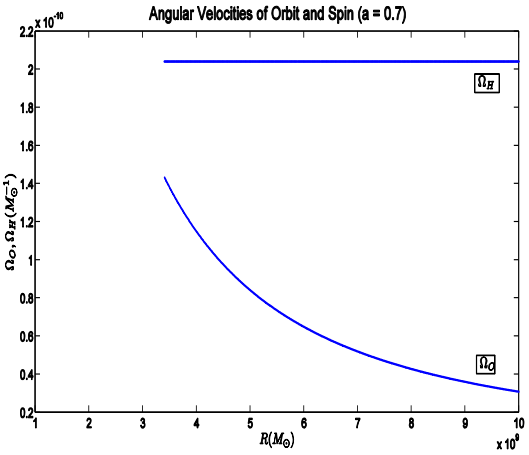

(m) When $R > R_{ISCO}$, $\Omega_H > \Omega_O$

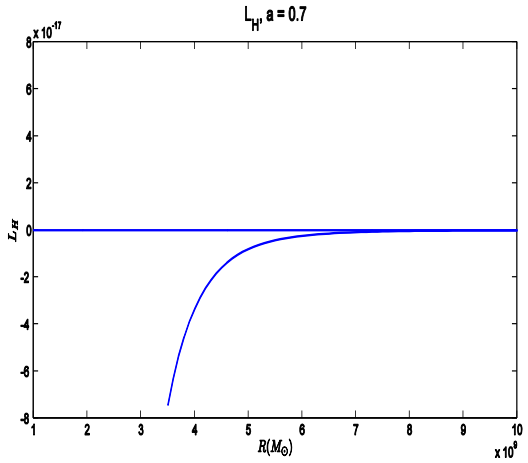

(n) When $R > R_{ISCO}$, $L_H < 0 \Rightarrow$ Superradiance

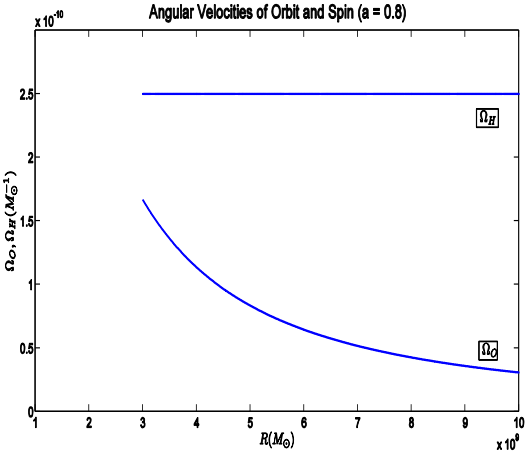

(o) When $R > R_{ISCO}$, $\Omega_H > \Omega_O$

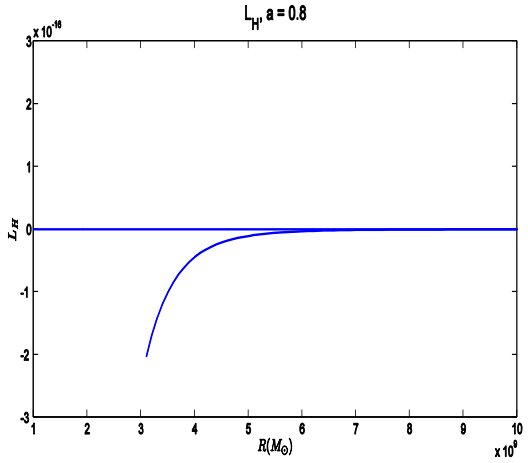

(p) When $R > R_{ISCO}$, $L_H < 0 \Rightarrow$ Superradiance

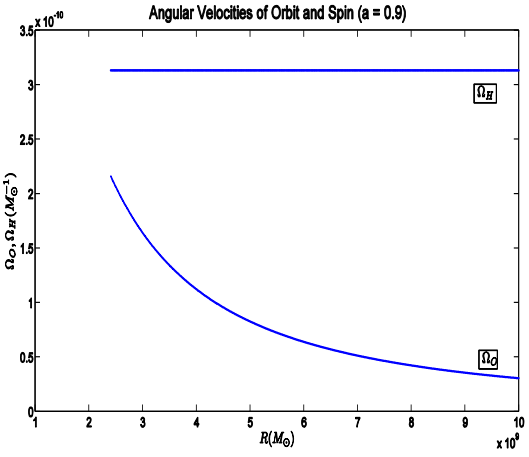

(q) When $R > R_{ISCO}$, $\Omega_H > \Omega_O$

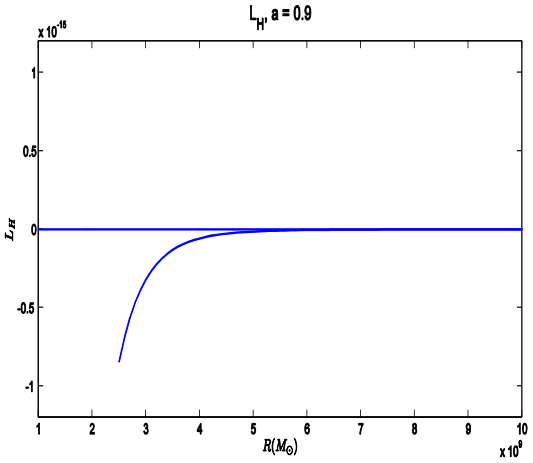

(r) When $R > R_{ISCO}$, $L_H < 0 \Rightarrow$ Superradiance

Figure 6: Evidence for the equivalence between superradiant scattering and tidal friction (cont.).

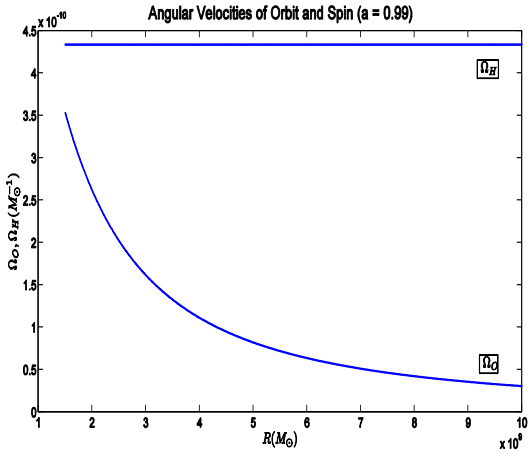

(s) When $R > R_{ISCO}$, $\Omega_H > \Omega_O$

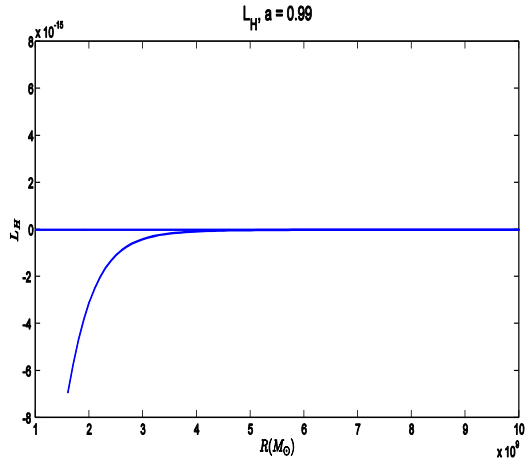

(t) When $R > R_{ISCO}$, $L_H < 0 \Rightarrow$ Superradiance

Figure 6: Evidence for the equivalence between superradiant scattering and tidal friction (cont.)

3.12 Floating Orbits Around Other Spinning Astrophysical Objects

Based on our numerical results, the maximum superradiant flux ratio ($Max\frac{|L_S|}{L_\infty}$) increases monotonically with the Kerr parameter a. For black holes, there are limitations on a , viz. $0 < a < 1$. However, the limitations are not the same for all astrophysical objects, and it is certainly of academic interest to ask whether floating orbits are possible around other astrophysical objects, with superradiant scattering/tidal friction as the mechanism for transferring spin energy to orbital energy. To determine the possibilities, we first need to find the value of a for which the superradiant flux ratio hits 100% . We therefore need to extrapolate using the data at hand (Fig: 4) and the polynomial used to fit the data points. The result is shown in Fig: 7.

While $a = 1.16$ cannot be achieved by black holes ($a_{max} = 1$) and neutron stars ($a_{max} \sim 0.7$ [23]), it may be possible for the still undiscovered quark stars to attain that value [23]. It is interesting to note that the earth has a Kerr parameter value that is significantly higher than the required $a = 1.16$. Let us estimate this value (in SI units) using elementary Newtonian mechanics. The earth has a spin angular frequency of $\omega = 7.29 \times 10^{-5} rad/s$, mass of $5.97 \times 10^{24} kg$ and a moment of inertia of $I = 8.04 \times 10^{37} kgm^2$ [21]. Its angular momentum is $J = I\omega$, and thus, $a = \frac{cJ}{GM^2} = 732$. The Kerr parameter for earth is much bigger than the required $a = 1.16$ for a floating orbit. And indeed we do observe a net gain in the moon's orbital energy at the expense of the earth's spin energy: its mean orbital radius increases at a rate of $38mm/yr$ [24] and the earth's day increases by $15\mu s/yr$ [24]. Thus we live in a system which is in a floating orbit, though no black hole is involved.

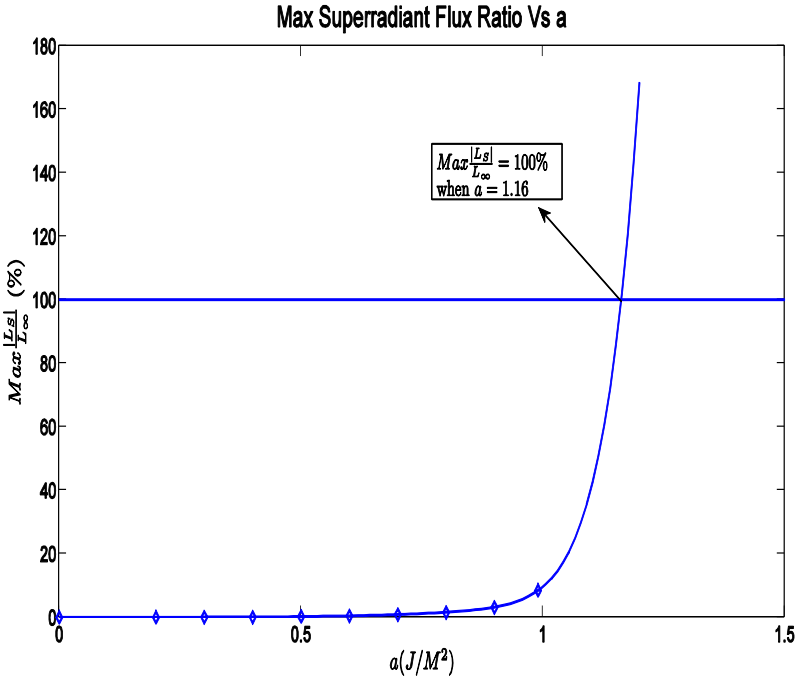

Figure 7: The extrapolated estimate (using a 12th degree polynomial fit) for the Kerr parameter a that gives a 100% max flux ratio is $a = 1.16$

4 Tidal Friction

4.1 Introduction

As previously mentioned, tidal friction is a mechanism equivalent to superradiant scattering that transfers spin energy to orbital energy. The works of Hartle and Poisson provide us with closed form expressions for the spin down (i.e, the rate of loss of spin angular momentum, $\dot{J}_{hole}$) of the black hole caused by tidal interaction with its companion body, valid under various limiting situations, such as a large orbital radius ($R >> M$) and/or extreme mass ratio ($m << M$) and/or slow rotation ($a << 1$). The spin energy lost by the black hole is then assumed to be completely transformed into orbital energy. This is expressed mathematically as:

$$\dot{E}_{orbital} = \Omega_{hole}\dot{J}_{hole} \tag{85}$$

Since we have algebraic expressions for the orbital energy flux gained, it is useful to get an analytical expression for the floating orbit radius by equating the flux gained to an analytical expression for the flux lost via graviational radiation to infinity (L_∞). This expression is often referred to as the quadrupole formula [27]:

$$L_Q = \frac{32}{5}\frac{(Mm)^2(M+m)}{R^5} \tag{86}$$

The quadrupole formula is an approximation for L_∞ that becomes increasingly accurate with increasing orbital radius, as shown in Fig: 8 and further illustrated in Fig: 9.

Thus, solving $\dot{E}_{orbital} = L_Q$ gives a rough estimate of the floating orbit radius. Eventually, $\dot{E}_{orbital} = L_\infty$ will have to be solved numerically to determine a more exact value for the floating orbit radius.

For the upcoming sections, we adopt the following notation: black hole of mass M has Kerr parameter a and black hole of mass m has Kerr parameter b, and R is the orbital radius that separates the black holes.

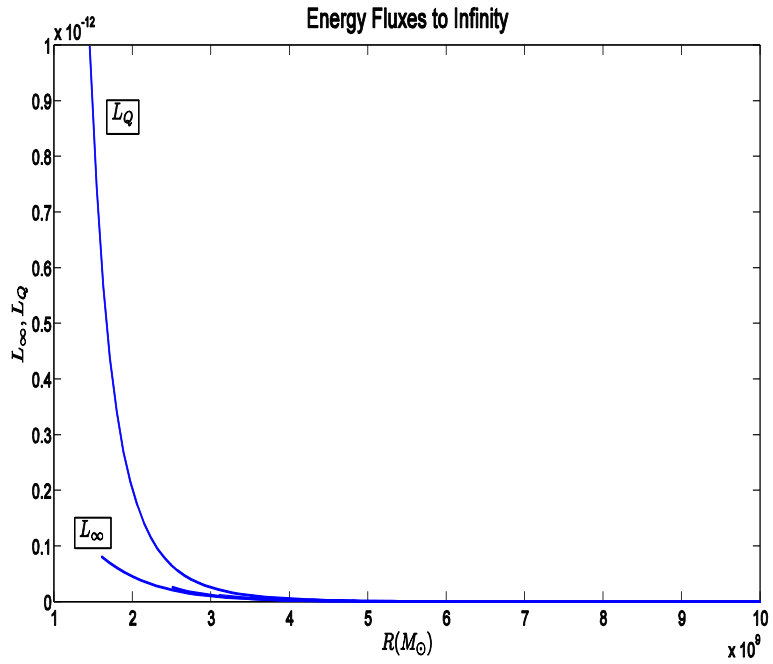

Figure 8: Both the quadrupole formula and L_∞ for $a = 0.1, 0.2, ...0.8, 0.9$ and 0.99 drop to zero asymptotically with increasing orbital radius.

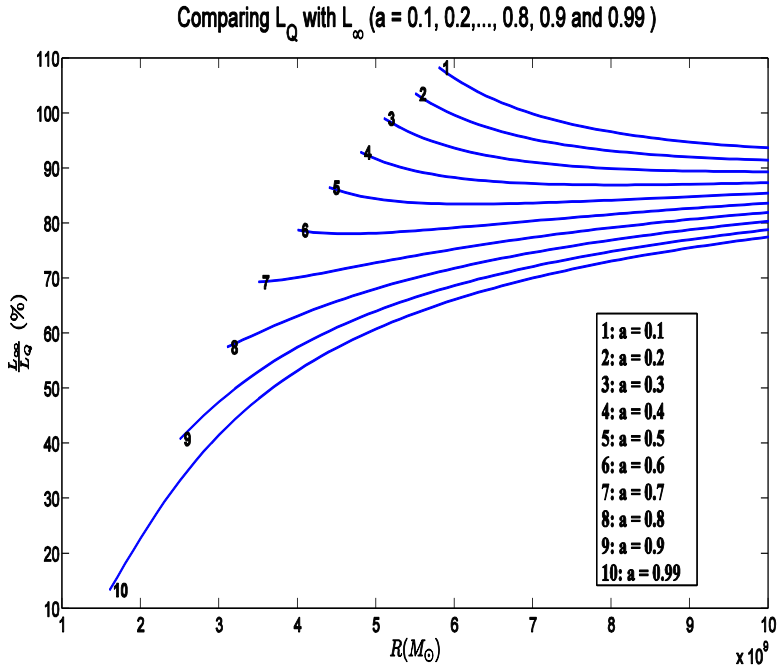

Figure 9: The figure suggests that $\frac{L_\infty}{L_Q}$ tends to 100% asymptotically with increasing orbital radius. However, for orbits close to the ISCO, the quadrupole formula becomes increasingly inaccurate, with $\frac{L_\infty}{L_Q}$ dropping below 20% near the ISCO radius for $a = 0.99$.

4.2 Binary Black Hole System with $m << M$, $0 < a << 1$ and $b = 0$

Consider an extreme mass ratio binary black hole moving in circular equatorial orbits. The larger black hole, with mass M and Kerr parameter $a << 1$, spins down via tidal interaction with its smaller satellite black hole of mass $m << M$. The black holes are separted by a large orbital radius $R >> M$.

The rate of change of the black hole's spin angular momentum due to tidal friction is given by [13]:

$$\dot{J}_1 = \frac{2}{5}\frac{Jm^2M^3}{R^6} \tag{87}$$

Converting (87) to a spin energy loss rate equation using (85) yields:

$$\dot{E}_1 = \frac{a^2m^2M^4}{5R^6(1+\sqrt{1-a^2})} \tag{88}$$

This is the spin energy loss rate of the rotating black hole, or, equivalently, the gain in orbital energy of the particle. Equating (88) with (86), we find the floating orbit radius as a function of the Kerr parameter:

$$R_{F1} = \frac{a^2}{32(1+\sqrt{1-a^2})}M \tag{89}$$

Fig: 10 shows the position of the floating orbit radius in contrast to the ISCO and event horizon radii. Not only have both the slow rotation and large orbital radius approximations been strained, the floating orbit radius turns out to be smaller than the event horizon radius of the larger black hole. We therefore need to find an expression for the orbital energy flux gain without limitations on the Kerr parameter or the size of the orbital radius.

4.3 Binary Black Hole System with $0 < a < 1$, $b = 0$ and $R >> m$

Consider the case of a spinning black hole of mass M and Kerr parameter a orbiting in the weak gravitational field of another mass m, with large orbital radius $R >> M$. The orbit is circular and equatorial. From [16], the rate of change of the black hole's spin angular momentum is:

$$\dot{J}_2 = \frac{8}{5}\eta^2\left(\frac{M}{M+m}\right)^2(M+m)a(1+3a^2)V^{12} \tag{90}$$

where $\eta = \frac{Mm}{(M+m)^2}$ and $V = \sqrt{\frac{M+m}{R}}$. The corresponding energy loss rate, found using (85), is:

$$\dot{E}_2 = \frac{4}{5}\frac{a^2(1+3a^2)M^4m^2}{R^6(1+\sqrt{1-a^2})} \tag{91}$$

Equating (91) with (86), we find the floating orbit radius to be:

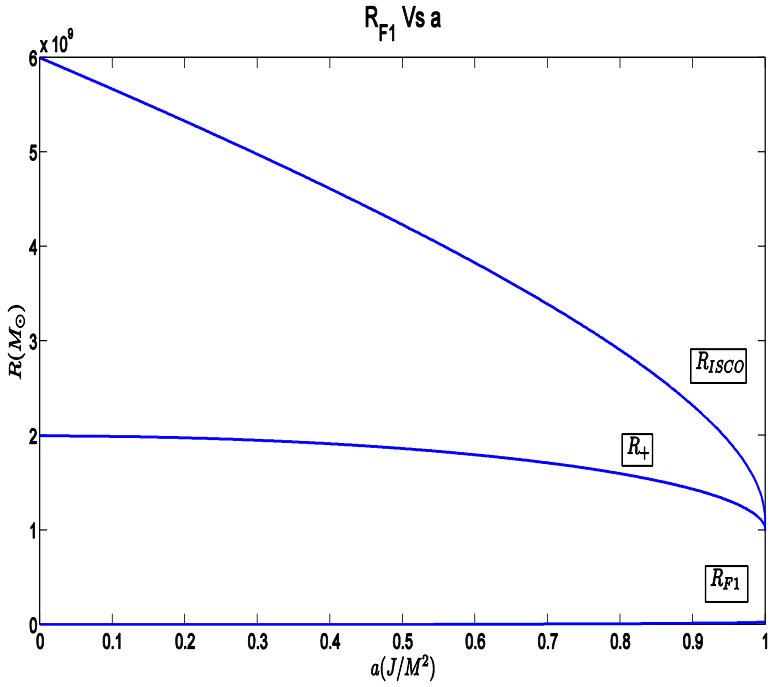

Figure 10: Clearly, the floating orbit radius R_{F1}(barely visible here, since it is very close to the x-axis) is smaller than the event horizon radius R_+ for all possible values of the Kerr parameter of the larger spinning black hole.

$$R_{F2} = \frac{a^2(1+3a^2)}{8(1+\sqrt{1-a^2})}\frac{M^2}{M+m} \tag{92}$$

R_{F2} is maximized in the extreme mass ratio case of $m << M$. The resulting expression for the floating orbit radius is:

$$R_{F2} = \frac{a^2(1+3a^2)}{8(1+\sqrt{1-a^2})}M \tag{93}$$

Fig: 11 shows the position of the floating orbit radius in contrast to the ISCO and event horizon radii. The floating orbit radius calculated using (91) turns out once again to be smaller than the event horizon radius of the larger black hole.

Relaxing the constraint on a did not help in maintaining the large orbital radius constraint required by (91), giving us a floating orbit inside the event horizon. We therefore need to remove the constraint on the orbital radius R as well.

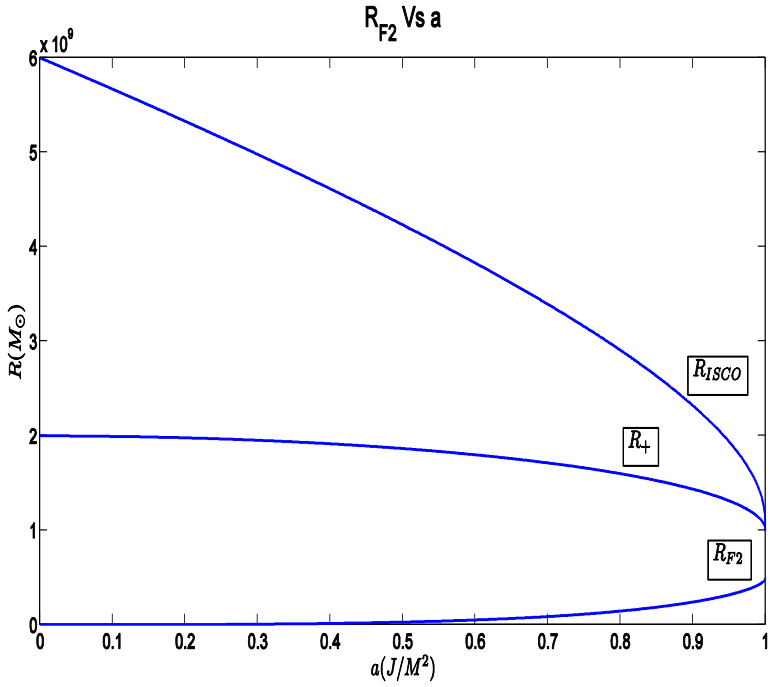

Figure 11: Clearly, the floating orbit radius R_{F2} is smaller than the event horizon radius R_+ for all possible values of the Kerr parameter of the spinning black hole.

4.4 Binary Black Hole System with $a = 0$, $0 < b < 1$, $m << M$ and $R \geq R_{ISCO}$

Consider the case of a small spinning black hole ($0 < b < 1$) of mass m in a circular equatorial orbit ($R > R_{ISCO}$) about a larger non spinning black hole of mass M. From [16], the rate of change of the black hole's spin angular momentum is

$$\dot{J}_3 = \frac{8}{5}\left(\frac{m}{M}\right)^5 Mb(1+3b^2)V^{12}\frac{(1-2V^2)(1-\frac{4+27b^2}{4+12b^2}V^2)}{(1-3V^2)^2} \tag{94}$$

where $V = \sqrt{\frac{M}{R}} \leq V_{ISCO} = 1/\sqrt{6}$. This condition on V is equivalent to $R \geq R_{ISCO}$

Using (85), the corresponding spin energy loss rate is found to be:

$$\dot{E}_3 = \frac{4}{5}\left(\frac{m}{M}\right)^5 (1+3b^2)V^{12}\frac{(1-2V^2)(1-\frac{4+27b^2}{4+12b^2}V^2)}{(1-3V^2)^2}\frac{b^2}{1+\sqrt{1-b^2}} \tag{95}$$

We could, in principle, equate (95) with (86) and calculate the floating orbit radius. However, in practice, this proves to be messy, given the rather complicated nature of (95). A simpler approach would be to determine the maximum possible value of $\dot{E}_3$ (which we call $\dot{E}_3^{max}$), and solve for the floating orbit radius using $\dot{E}_3^{max}$.

Fig: 12 suggests that $\dot{E}_3^{max}$ occurs when both V and b are maximized, i.e, $V = V_{ISCO}$ and $b = 1$. A

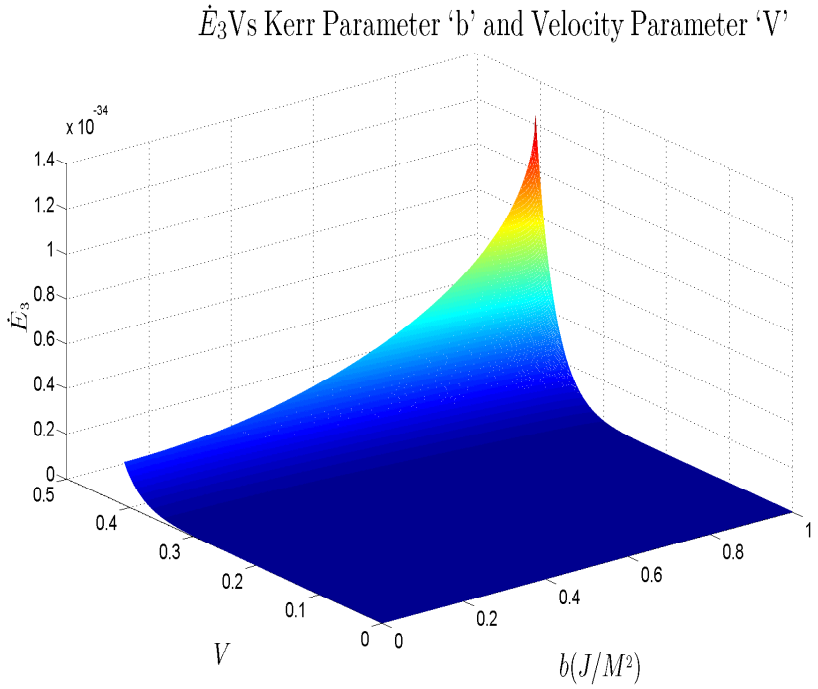

Figure 12: According to the figure, the gain in orbital energy flux is a maximum at the ISCO where $V = V_{ISCO}$, and $b = 1$.

simple calculation then yields $\dot{E}_3^{max} = 1.24 \times 10^{-4} \times (m/M)^5$.

Writing the quadrupole formula (86) in terms of V in the extreme mass ratio ($m << M$) case:

$$L_Q = \frac{32}{5}\left(\frac{m}{M}\right)^2 V^{10}, \tag{96}$$

we find that, at the ISCO, $L_Q = 8.23 \times 10^{-4} \times (m/M)^2$.

It is clear that $\dot{E}_3^{max}$ scales as $(m/M)^5 \sim 10^{-30}$, far less than L_Q, which scales as $(m/M)^2 \sim 10^{-12}$. There is however one radius R_{F3} at which (95) blows up, helping $\dot{E}_3^{max}$ to scale up to L_Q, and thus potentially allowing a floating orbit:

$$R_{F3} = 3M \tag{97}$$

This radius, though greater than the event horizon radius $R_+ = 2M$ of the larger non spinning balck hole, is smaller than the ISCO radius $R_{ISCO} = 6M$ (Fig: 13)

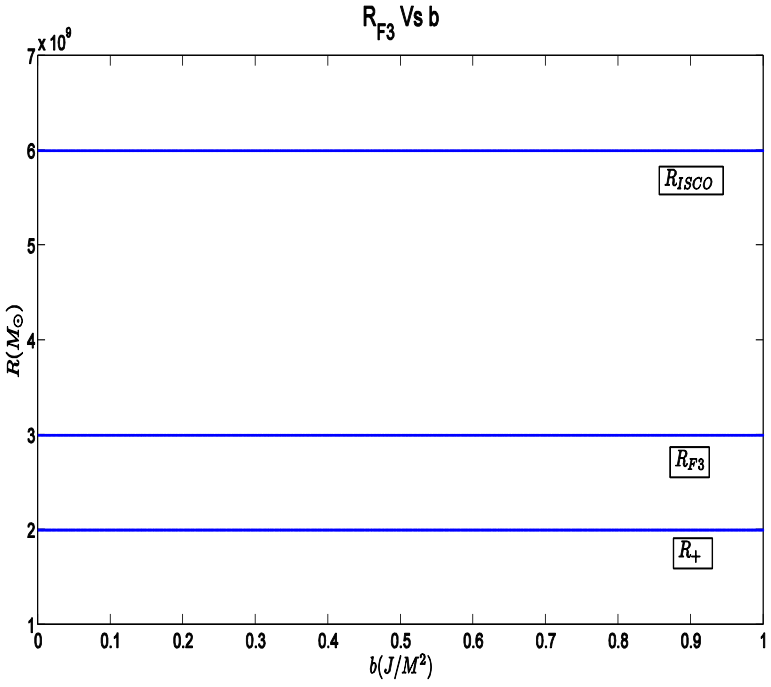

Figure 13: Clearly, $R_+ < R_{F3} < R_{ISCO}$.

4.5 Binary Black Hole System with $0 < a < 1$, $0 < b < 1$, $m << M$, and $R \geq R_{ISCO}(a)$

We now allow both black holes in the binary system to spin. The larger black hole of mass M has Kerr parameter a and the smaller black hole of mass m has Kerr parameter b. There are no restrictions on either Kerr parameter ($0 < a < 1$, $0 < b < 1$) and the orbital radius ($R > R_{ISCO}$).

From [17], the rate of change of the smaller black hole's spin angular momentum is given by

$$\dot{J}_4 = \frac{8}{5}\frac{m^5}{M^4} b(1+3b^2)V^{12}\frac{1-2V^2+a^2V^4}{(1-3V^2+2aV^3)^2}(1-\frac{4+27b^2}{4+12b^2}V^2-\frac{4-3b^2}{2+6b^2}aV^3+\frac{8+9b^2}{4+12b^2}a^2V^4) \tag{98}$$

The corresponding spin energy loss rate is, from (85):

$$\begin{aligned}\dot{E}_4 &= \frac{4}{5}\frac{m^5}{M^5}(1+3b^2)V^{12}\frac{1-2V^2+a^2V^4}{(1-3V^2+2aV^3)^2}(1-\frac{4+27b^2}{4+12b^2}V^2 \\ &- \frac{4-3b^2}{2+6b^2}aV^3+\frac{8+9b^2}{4+12b^2}a^2V^4)\frac{b^2}{1+\sqrt{1-b^2}}\end{aligned} \tag{99}$$

with $V = \sqrt{\frac{M}{R}} < V_{ISCO}(a)$.

We may also write (99) as:

$$\dot{E}_4 = \frac{4}{5}\frac{m^5}{M^5}(1+3b^2)V^{12}\Gamma_K\frac{b^2}{1+\sqrt{1-b^2}} \tag{100}$$

where

$$\Gamma_K(a,b,V) = \frac{1-2V^2+a^2V^4}{(1-3V^2+2aV^3)^2}(1-\frac{4+27b^2}{4+12b^2}V^2-\frac{4-3b^2}{2+6b^2}aV^3+\frac{8+9b^2}{4+12b^2}a^2V^4) \tag{101}$$

is the "relativistic factor" [17]. It turns out that the relativistic factor becomes independant of a in the limiting case when the velocity parameter tends towards its ISCO value [17]:

$$V \to V_{ISCO} \Rightarrow \Gamma_K(a,b,V_{ISCO}(a)) = \frac{5}{9}\frac{4+9b^2}{1+3b^2} \equiv \Gamma_K(b) \tag{102}$$

The maximum value that the relativistic factor can take is $\Gamma_K(b=1) = 65/36$. Using this value, the maximum value that $\dot{E}_4$ can take is found to be $\dot{E}_4^{max} = (52/9)\times(m/M)^5$, when $a=1$ and $V = V_{ISCO}(a=1)$. At the ISCO of an extremally spinning black hole ($a=1$), the quadrupole formula assumes the value $L_Q = 32/5\times(m/M)^2$ (cf (86)).

Like in the previous case where the larger black hole was not spinning (which is simply the current case for $a=0$), $\dot{E}_3^{max}$ scales as $(m/M)^5$, far less than the quadrupole formula L_Q, which scales as $(m/M)^2$

For there to be any hope of (99) scaling as (96), we must require the denominator $(1-3V^2+2aV^3)^2$ in (99) to drop to a value close to zero: (An example of this is shown in Fig: 14 for $a=0.99$).

$$(1-3V^2+2aV^3)^2 = 0 \tag{103}$$

The solution of (103), which is the floating orbit radius R_{F4} is plotted in Fig: 15, as a function of the Kerr parameter a of the larger black hole.

Fig: 15 clearly shows that for all values of the Kerr parameter a of the larger black hole, the floating orbit radius does not exceed the radius of the ISCO. However, for the extremally spinning case of $a=1$, the floating orbit radius equals both the ISCO radius and the event horizon radius ($R_+ = R_{F4} = R_{ISCO} = M$). This in itself is not a convincing argument for the existence of a floating orbit, since, at the event horizon, the orbital velocity must equal the speed of light for the orbit to be stable. Furthermore, for $R = R_{F4} = M$, (99) does NOT blow up. This is simply because at the ISCO, the relativistic factor Γ_K assumes a limiting value (cf (102)), and for an extremally spinning black hole, $R = M$ is the ISCO radius.

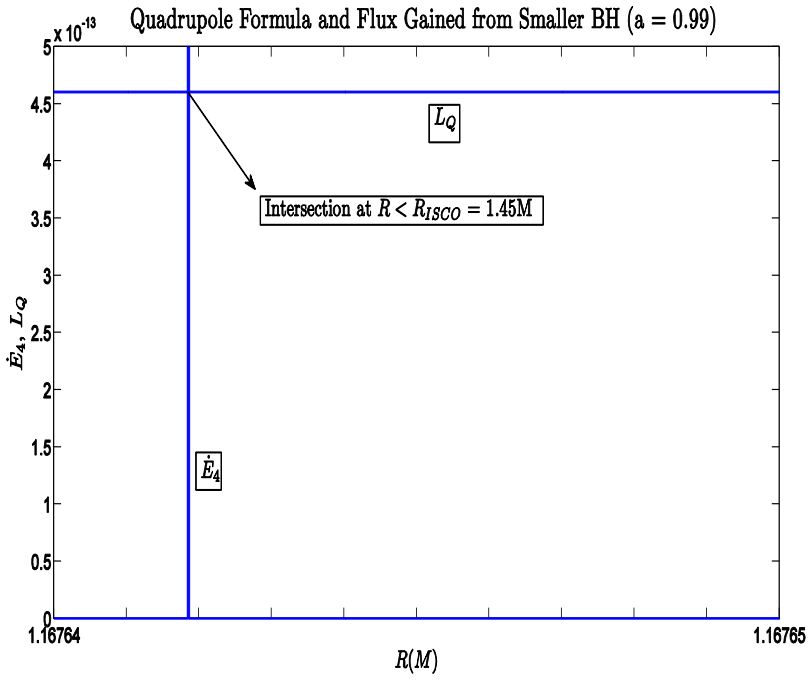

Figure 14: The flux gained from the smaller black hole blows up, and thus scales up to the quadrupole formula. However, this occurs within the ISCO.

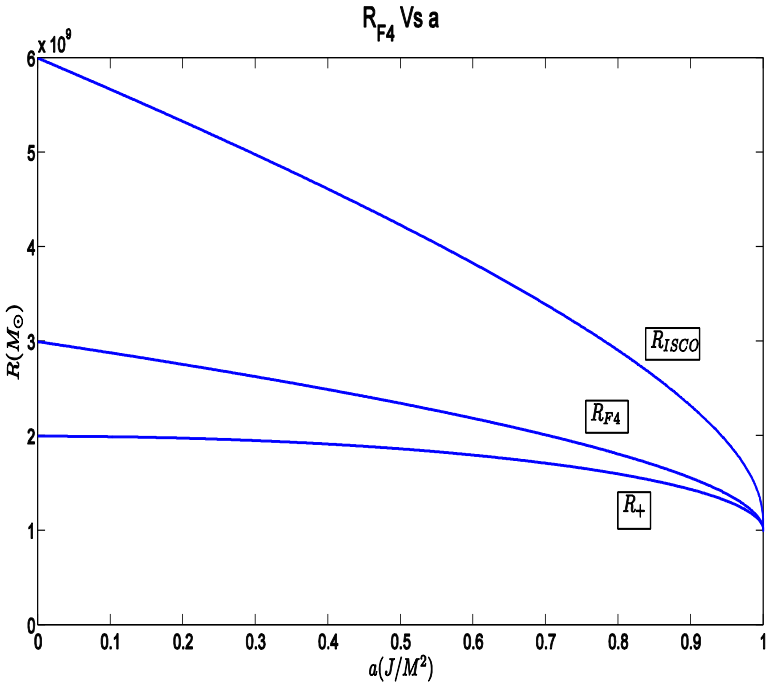

Figure 15: Once again, $R_+ < R_{F4} < R_{ISCO}$, except for $a = 1$ where $R_+ = R_{F4} = R_{ISCO} = M$

Mathematically, when the larger black hole is extremally spinning, $R = M$ and $V_{ISCO} = 1$, and therefore both the numerator and denominator of the relativistic factor Γ_K (cf (100)) hit zero. The result is that Γ_K does not blow up, and $\dot{E}_4$ does not scale up to the quadrupole formula at $R = M$

The above analysis strongly suggests that the spin energy extracted from the smaller black hole is not enough to replenish the orbital energy lost by the binary system to infinity. However, the calculations approximated the energy flux radiated to infinity (L_∞) by the quadrupole formula (L_Q), which, for a rapidly spinning black hole ($a = 0.99$ for example), greatly overestimates the energy flux to infinity for orbits close to the ISCO (cf Fig: 9).

A comparison of the scalings of the ratio of the fluxes,

$$\frac{\dot{E}_4}{L_Q} \sim \left(\frac{m}{M}\right)^3 = 10^{-18} \text{ and } \frac{\mathrm{L}_\infty}{\mathrm{L}_\mathrm{Q}} \sim 1 \tag{104}$$

suggests that $\frac{\dot{E}_4}{L_\infty} \sim 10^{-18}$. This is confirmed in Fig: 16.

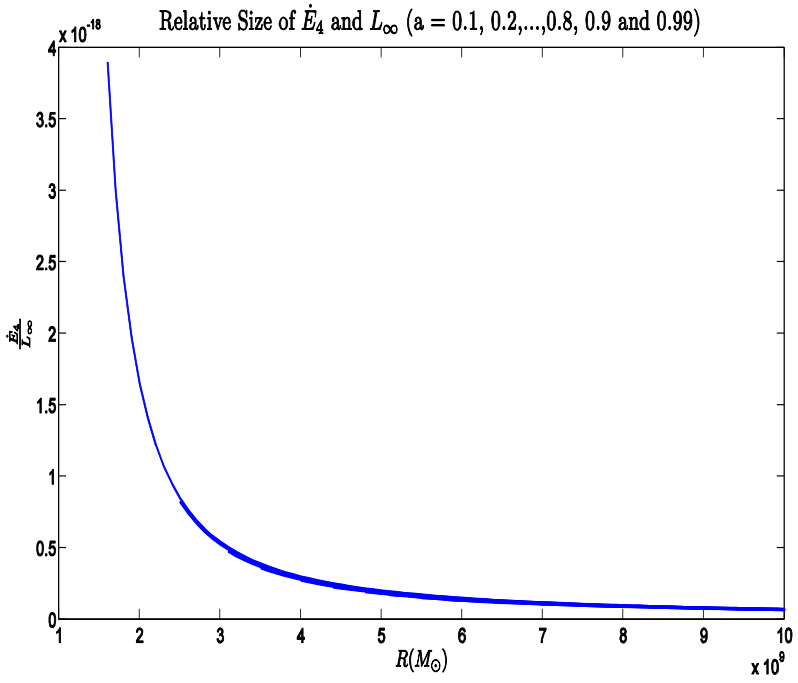

Figure 16: As expected, $\frac{\dot{E}_4}{L_\infty} \sim \frac{\dot{E}_4}{L_Q} \sim \left(\frac{m}{M}\right)^3 = 10^{-18}$.

Using a more exact numerical value for L_∞ rather than its rough algebraic estimate L_Q does not change the central result of this section, which is, that the spin energy extracted from the smaller black hole via tidal friction is not enough to generate a stable floating orbit.

5 Combining Both Approaches

Neither superradiant scattering nor tidal friction were in themselves adequate to generate a floating orbit for extreme mass ratio binary black holes.

Superradiant scattering provided a means to calculate the orbital energy gained by the extraction of spin energy from the larger black hole. However, we were unable to use this mechanism to calculate the orbital energy gained from the smaller black hole's spin energy (In superradiant scattering, the orbiting particle was non-spinning). On the other hand, tidal friction provided a way to calculate the orbital energy gained by the extraction of spin energy from the smaller black hole. But this time, we were unable to use this mechanism to calculate the orbital energy gained from the large black hole.

Nonetheless, as asserted earlier, superradiant scattering and tidal friction are equivalent mechanisms - they are just two ways of expressing the same process. Therefore, to calculate the total orbital flux gained from the spins of both black holes, we simply add the orbital energy fluxes gained from both black hole spin energies (cf Sections 3.9 and 4.5):

$$L_T = |L_S| + \dot{E}_4 \tag{105}$$

For a floating orbit to exist, we need to examine the ratio L_T/L_∞. If this ratio reaches 100% for a certain orbital radius greater than the ISCO radius, we would have a floating orbit.

Looking at the order of magnitude $\dot{E}_4$ in comparison to that of L_H suggests that $L_H >> \dot{E}_4$. This is illustrated in Fig: 17 and Fig: 18.

The superradiant flux L_S was previously defined as equal to L_H when $L_H < 0$, and zero otherwise (cf (65)). From Fig: 18, $L_T \simeq |L_S|$. The maximum possible superradiant flux ratio (i.e, the maximum possible value of $|L_S|/L_\infty$) does not exceed 10% (cf Section 3.9). Thus, we don't expect L_T/L_∞ to exceed 10% either.

Fig: 19 plots the ratio of the maximum total orbital flux gain to the orbital flux lost ($Max\frac{L_T}{L_\infty}$) for different values of the Kerr parameter a of the larger black hole. The Kerr parameter b of the smaller black hole is set to 1, because the orbital flux gained from the smaller black hole is maximized when it is extremally spinning. Indeed, as anticipated, L_T/L_∞ does not exceed 10%, much less than the required 100%.

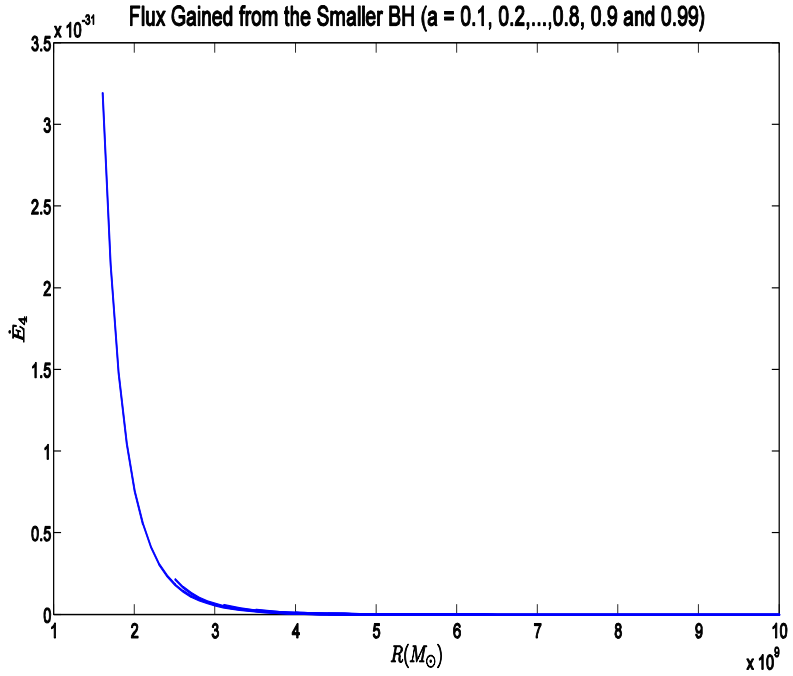

Figure 17: The orbital flux gain from the smaller black hole is several orders of magnitude smaller than the flux gain from the larger black hole (cf Fig: 2).

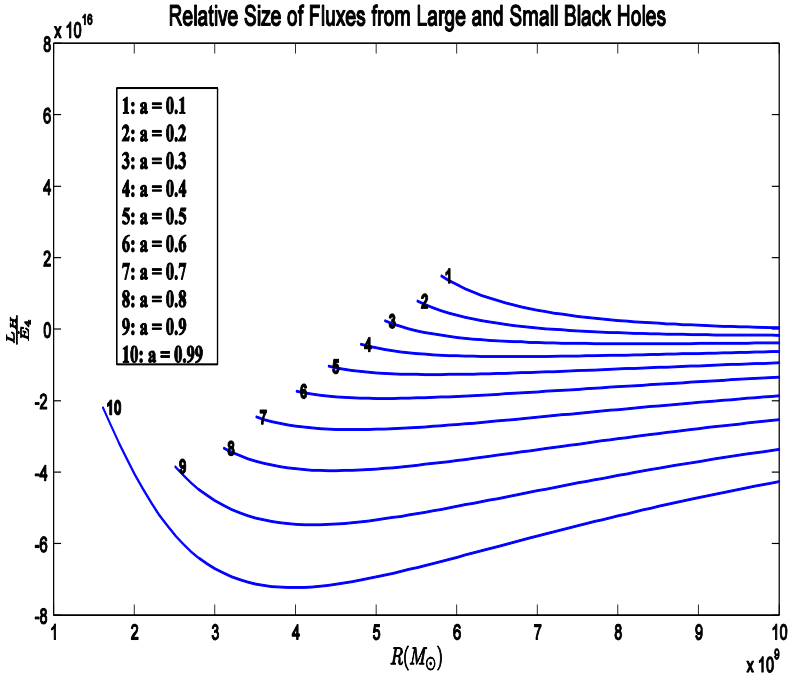

Figure 18: Clearly, the energy flux from the larger black hole is about sixteen orders of magnitude greater than the flux from the smaller black hole. Therefore, $|L_S|/\dot{E}_4 >> 1$ and $L_T = |L_S| + \dot{E}_4 \simeq |L_S|$.

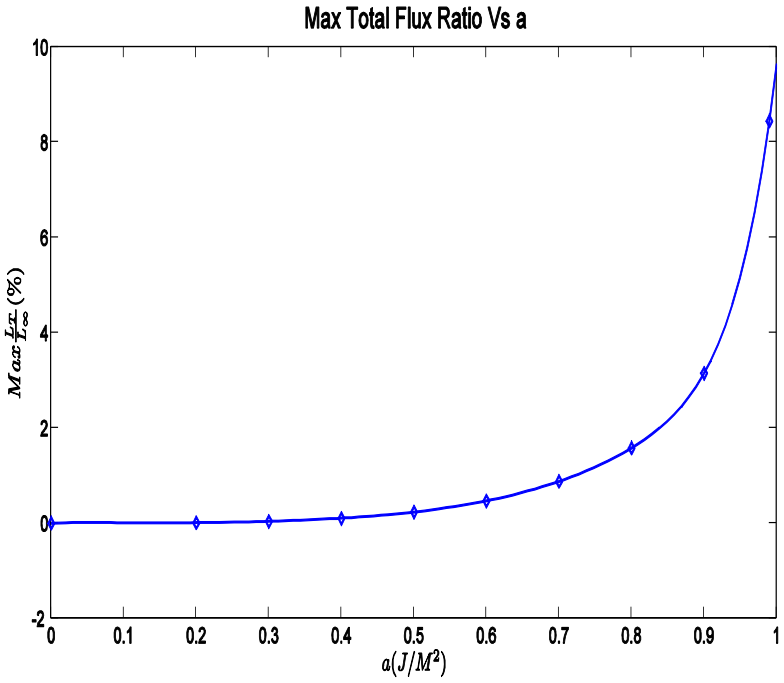

Figure 19: As anticipated, the extrapolated estimate (using a 12th degree polynomial fit) for the magnitude of the maximum possible total flux ratio $\frac{L_T}{L_\infty}$ does not exceed 10%.

Fig: 19 makes it clear that, for extreme mass ratio binary black holes in circular equatorial orbits outside the ISCO, the orbital energy flux radiated away to infinity exceeds the sum of the fluxes gained from the spins of both black holes. Thus, stable floating orbits generated via extraction of the spin energies of the black holes are a physical impossibility. This is the central result of our thesis.

6 Conclusion and Scope for Future Work

6.1 Conclusion

The thesis concerned itself with circular equatorial orbits for extreme mass ratio binary black holes, and the numerical calculations assumed $m = 10^3 M_\odot$ and $M = 10^9 M_\odot$.

For such orbits, the orbital energy gained from the spin energy of the larger black hole ($|L_S|$) was less than 10% of the energy radiated away to infinity (L_∞). This was found by employing the superradiant scattering formalism.

On the other hand, the orbital energy gained from the spin energy of the smaller black hole ($\dot{E}_4$) was found to scale as $(m/M)^5$, much smaller than the orbital energy radiated away, which scales as $(m/M)^2$ ($L_Q \sim L_\infty$). This was found by employing the tidal friction formalism.

Adding the orbital energies gained from both black holes ($L_T = L_H + \dot{E}_4$) and comparing it to the orbital energy radiated away reveals that the ratio of the energy gained to the energy lost is still less than 10% ($L_T/L_\infty < 10\%$).

Tidal friction and superradiant scattering are two different ways of looking at the same mechanism of converting black hole spin energy to orbital energy. While this is not formally proven, the thesis does give striking evidence of this equivalence by finding a clear correspondence between the relative magnitude of the angular velocities of orbit and spin, which is dependant on the orbital radius, and the occurrence of superradiant scattering, which is also dependant on orbital radius.

Assuming both formalisms describe the same spin energy extracting process, it is clear that this mechanism is unique. Therefore, in calculating the energy extracted from the two spinning black holes in a binary, we are finding the maximum possible energy which can be converted into orbital energy in this system. Thus, the orbital energy gained from stealing spin energy of both black holes never exceeds the orbital energy lost. This leads to the central conclusion of this thesis, which is that circular equatorial floating orbits for extreme mass ratio binary black holes cannot exist.

6.2 Eccentric and Non-Equatorial Orbits

We have so far assumed circular equatorial orbits. These are obviously not the most general possible orbits, but are in fact a particular kind of eccentric orbit, with eccentricity $e = 0$. To our knowledge, there is no closed form expression for the flux gained from the smaller or larger black hole, for arbitrary eccentricity, in the tidal friction paradigm. In the superradiant scattering picture, the code used to calculate the fluxes to infinity (L_∞) and the horizon (L_H) works reasonably well for low eccentricities but crashes for high eccentricities. To get a clear pattern of how eccentricity affects the two fluxes, the code needs to be modified

to handle higher eccentricities. Nonetheless, the code was run for certain eccentricities (and $a = 0.99$), and the results are shown in Fig: 20, 21, and 22.

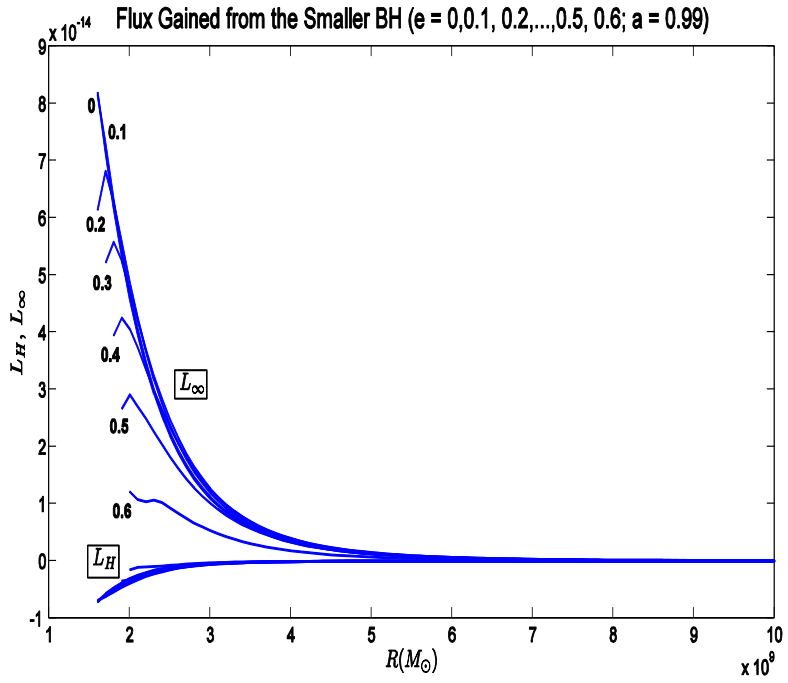

Figure 20: L_∞ and L_H are plotted for various values of e. Here, R are denotes the semi latus rectum of the ellipitc orbits. For all eccentricities shown, the flux L_∞ is still much greater than L_H. Note the sudden dip in certain curves. These occur because of a change in eccentricity which causes a drop in the flux [12].

Fig: 20 shows that $|L_S| < L_\infty$ (L_S was defined earlier in Section 3.9). Fig: 21 further illustrates this, suggesting that the ratio of the fluxes L_H/L_∞, and thus $|L_S|/L_\infty$, is within 20%, far less than the required 100%. Fig: 22 shows how the maximum superradiant flux ratio for a given e varies with e. Unlike for the variation of this ratio with a which increased monotonically with increasing a (cf Fig: 4), its non-monotonic variation with e makes determining the maximum possible value of this ratio harder, and requires more data points at higher eccentricities. Nonetheless, Fig: 22 seems to indicate that this maximum value will still be comfortably less than 100%. We would also need to add $|L_S|$ to the flux gained from the spin of the smaller black hole $\dot{E}_4$. However, if the results of the previous section which suggested that $L_\infty \sim L_Q \sim (m/M)^2$ and $\dot{E}_4 \sim (m/M)^5$ are any indication, we would still have $L_T/L_\infty < 20\%$. There is therefore no real reason to believe that for an eccentricity e different from zero, a floating orbit may exist.

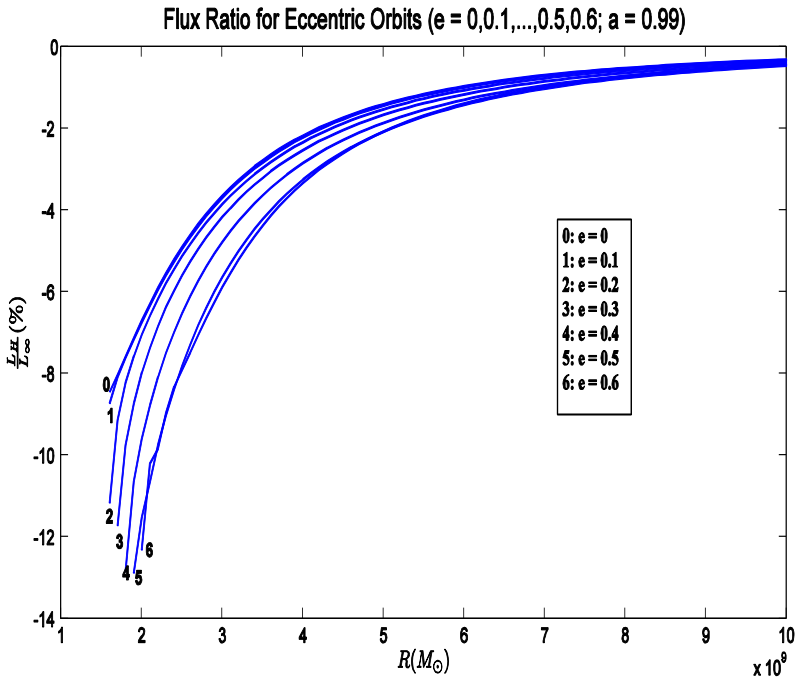

Figure 21: The ratio L_H/L_∞ is plotted for various eccentricities. This ratio, and thus the superradiant flux ratio $|L_S|/L_\infty$, is within 20% for all eccentricities used.

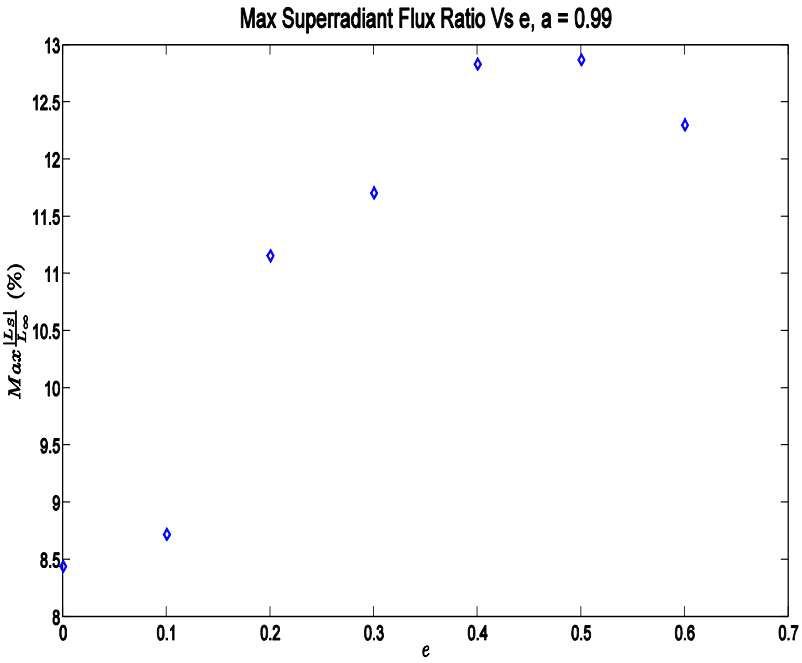

Figure 22: The maximum superradiant flux ratio does not vary monotonically with eccentricity. The lack of data points for higher eccentricities makes it difficult to predict the maximum possible flux ratio. Nonetheless, the data points in this plot strongly suggests that this ratio will never exceed 100%.

The code used for this thesis is currently not capable of computing fluxes (L_H and L_∞) for non-equatorial orbits using superradiant scattering, and, to our knowledge, there is no expression in the literature for the orbital flux gained from the smaller black hole or larger black hole, for non-equatorial orbits. [15] studies the evolution of circular non-equatorial orbits using the superradiant scattering picture and, from the results of that paper, which specifically considered the possibility of floating orbits, there doesn't seem to be any indication that inclined orbits are more likely to facilitate floating orbits than are equatorial orbits.

6.3 The Relevance of Floating Orbits in the Search for Gravitational Waves

Gravitational waves, as predicted by general relativity, are ripples in spacetime that carry energy. They play an important role in the motion of binary systems, such as binary black holes and binary neutron stars, since they radiate away orbital energy at rates that are significant with respect to the orbital period. However, gravitational waves have so far not been detected on earth. Large scientific experiments, such as the ongoing ground based LIGO (Large Interferometer Gravitational Wave Observatory) and the proposed space based LISA (Laser Interferometer Space Antenna), hope to detect these waves in the near future.

Supermassive black holes ($\sim 10^9 M_\odot$), orbited by smaller black holes ($\sim 10^3 M_\odot$), are expected to be possible sources of detectable gravitational waves, and are also probably the most scientifically interesting from the point of view of astrophysics and cosmology. Furthermore, if they were to form floating orbits, the emitted waves would maintain a constant frequency. Such waves would show up as delta function-like peaks in frequency space, thus clearly standing out from the background noise.

This thesis strongly suggests that floating orbits as a source for constant frequency gravitational waves are not possible. However, the thesis also shows that the spin energy of the black holes converted to orbital energy of the binary, while not enough to generate a floating orbit, is a significant percentage ($\sim 10\%$) of the orbital energy radiated away. Therefore, any analysis involving trajectories of binary black holes spiralling into each other must consider the effects of superradiant scattering/tidal friction.

References

[1] J.Weber, Phys. Rev. Lett. 25, 180 (1970).

[2] C. Misner, Phys. Rev. Lett. 28, 994 (1972).

[3] J.D.Jackson, Classical Electrodynamics, (John Wiley and Sons, 1999).

[4] S. Gillessen; F. Eisenhauer; S.Trippe; T. Alexander; R.Genzel; F. Martins; T. Ott, The Astrophysical Journal 692, 1075 (2009).

[5] D.J. Majaess; D.G.Turner, D.J.Lane, MNRAS 398, 263 (2009)

[6] D.W.Sciama; G.B.Field; M.J.Rees, Phys. Rev. Lett. 23, 1514 (1969)

[7] A.Frebel; N. Christlieb; J. Norris; C. Thom; T. Beers; J. Rhee The Astrophysical Journal 660, L117 (2007)

[8] J.McMillan, MNRAS 414, 2446 (2011)

[9] W. Press; S.Teukolsky, Nature 238, 211 (1972)

[10] S.Teukolsky, The Astrophysical Journal 185, 635 (1973)

[11] S.Detweiler, The Astrophyscal Journal 225, 687 (1978)

[12] K. Glampedakis; D. Kennefick, Phys. Rev. D 66, 044002 (2002)

[13] J.Hartle, Phys. Rev. D 8, 1010 (1973)

[14] K.Thorne; R.Price; D.Macdonald, "Black Holes: The Membrane Paradigm" (Yale University Press, New Haven, CT, 1986)

[15] S.Hughes, Phys. Rev. D 64, 064004 (2001)

[16] E. Poisson, Phys. Rev. D 70, 084044 (2004)

[17] S. Comeau, E. Poisson, Phys. Rev. D 80, 087501 (2009).

[18] M. Sasaki; H. Tagoshi, "Analytic Black Hole Perturbation Approach to Gravitational Radiation", http://www.livingreviews.org/lrr-2003-6

[19] E. Poisson, Phys. Rev. D 47, 1497 (1993)

[20] G.Arfken, H.Weber, "Mathematical Methods for Physicists" (Elsevier Academic Press, 2005)

[21] J.Hartle, “Gravity”, (Pearson Education, Inc, 2003)

[22] S. Teukolsky, W. Press, The Astrophysical Journal 193, 443 (1974)

[23] K.Lo, L.Lin, The Astrophysical Journal 728, 12 (2011)

[24] J. Chapront, M. Chapront-Touze, G. Francou, The Astrophysical Journal 387, 700 (2002)

[25] L. Fishbone, The Astrophysical Journal 185, 43 (1973)

[26] R.Wald, “General Relativity” (The University of Chicago Press, 1984)

[27] P.Peters, C.Matthews, Phys. Rev. Lett. 131, 435 (1963)